https://doi.org/10.1070/RCR4987

Redox flow batteries: role in modern electric power industry and comparative characteristics of the main types

Mikhail M. Petrov,[a, b]* Alexander D. Modestov,[c] Dmitriy V. Konev,[b] Anatoly E. Antipov,[a, b, c, d] Pavel A. Loktionov,[a, b] Roman D. Pichugov,[a, b] Natalya V. Kartashova,[a, d] Artem T. Glazkov,[a, b, c] Lilia Z. Abunaeva,[a, e] Vladimir N. Andreev,[c] Mikhail A. Vorotyntsev [c]

[a] *Mendeleev University of Chemical Technology of Russia, Miusskaya pl. 9, 125047 Moscow, Russian Federation*
[b] *Institute of Problems of Chemical Physics, Russian Academy of Sciences, prosp. Akademika Semenova 1, 142432 Chernogolovka, Moscow Region, Russian Federation*
[c] *Frumkin Institute of Physical Chemistry and Electrochemistry, Russian Academy of Sciences, Leninsky prosp. 31, 119071 Moscow, Russian Federation*
[d] *Lomonosov Moscow State University, Leninskie Gory 1, 119991 Moscow, Russian Federation*
[e] *Moscow Institute of Physics and Technology (National Research University), Institutskii per. 9, 141701 Dolgoprudnyi, Moscow Region, Russian Federation*

In recent years, the key principles of the electric power industry have radically changed and the number of studies on the development of devices for electrical energy storage in a different form such as mechanical or chemical energy has rapidly increased. This review gives a brief description of these devices. The attention is focused on redox flow batteries (RFBs), a promising type of energy storage devices capable of efficiently operating in distributed power grids, in order to eliminate the imbalance between the time-varying electricity production by 'unconventional sources' and electricity consumption. At the design level, RFBs combine the principles of fuel cells and chemical energy sources with solid electroactive materials: transitions between electrical and chemical forms of energy in these devices occur upon oxidation and reduction of redox-active electrolytes, which are stored in separate tanks and pumped into the electrode compartments of the membrane electrode assembly (MEA) separated by a semi-permeable membrane. This approach ensures an important advantage of these devices over other types of chemical energy sources, that is, the possibility of independent scaling of the energy storage capacity and power characteristics of the system. This review provides a systematic description of the main types of RFBs and analysis of their fundamental benefits and drawbacks, which determine the prospects for practical applications of RFBs. The bibliography includes 149 references.

Contents

1. Introduction 678
2. Electric power industry in the general energy consumption structure. Electrochemical power sources 679
2.1. Evolution of the energy consumption structure and of the role of electricity 679
2.2. Temporary storage of electricity as mechanical energy 680
2.2.1. Pumped storage hydroelectric power plant (PSHPP) 680
2.2.2. Kinetic energy storage 680
2.2.3. Pneumatic energy storage 680
2.3. Secondary/rechargeable electrochemical cells 681
2.3.1. Lithium-ion battery 681
2.3.2. Sodium sulfur battery 681
2.3.3. Sodium-nickel chloride battery 681
2.3.4. Lead battery 681
2.3.5. Electrochemical (super)capacitor 681
2.3.6. Flow and hybrid batteries 681
3. Redox flow batteries 682
3.1. Classical RFBs 682
3.1.1. All-vanadium RFB 682
3.1.2. Iron chromium RFB 683
3.1.3. Polysulfide halide RFB 683
3.1.4. Anthraquinone bromine RFBs 684
3.1.5. Miscellaneous organic RFBs 685
3.2. Hybrid RFBs, type I 687
3.2.1. Zinc bromine RFB 687
3.2.2. Other RFBs with zinc metal anode 688
3.2.3. Lithium redox flow battery 689
3.2.4. Hydrogen halogen RFB 690
3.3. Hybrid RFBs, type II 690
3.3.1. RFBs using redox mediators 690
3.3.2. Suspension RFBs 692
3.3.3. RFBs using additional flow circuits and/or cells 694
3.3.4. RFBs using auxiliary processes 696
4. Note added in proof 698
5. Conclusion 698
6. List of acronyms and designations 699

Received 31 July 2020

© 2021 Uspekhi Khimii, ZIOC RAS, Russian Academy of Sciences and IOP Publishing Limited

1. Introduction

The role of renewable energy sources has strongly increased in recent years, due to the global climate change and gradual depletion of fossil fuels based on hydrocarbons.[1] Simultaneously, there has been increased demand for stationary energy storage systems that can be combined with these energy sources to smooth down the irregular patterns of both production and consumption of electricity.

Currently, various devices are used for energy storage. Among them, the dominant position belongs to pumped storage hydroelectric power plants; however, they can be constructed only at large water areas in which a considerable elevation drop can be arranged.[2, 3] This fact, together with the high capital cost of construction of pumped storage hydroelectric power plants, leads to gradually decreasing role of this technology, being replaced by various chemical power sources (CPS), which store electrical energy as redox-active compounds.

Among the diversity of CPS (lithium-ion batteries, fuel cells, electrochemical capacitors), redox flow batteries (RFBs) appear especially relevant to large-scale stationary energy storage. These devices generate electricity by oxidation and reduction of redox-active electrolytes, which are stored in separate tanks and are circulated through membrane-separated electrode compartments of the membrane electrode assembly (MEA).[4] At the design level, RFBs combine the principles of fuel cells and lithium-ion batteries. This approach gives them an important advantage over other types of CPS, that is, independent scalability of power characteristics (determined by MEA parameters) and capacity characteristics (determined by the electrolyte composition and the volume of tanks) of the storage device.

A typical RFB is the vanadium redox flow battery using solutions of vanadium salts as electrolytes.[5] Many other commercialized types of RFB operate in a similar way, *e.g.*, polysulfide bromide or iron chromium flow batteries. In the present review, all these types are designated as classic RFBs and are briefly considered in Section 2.1.

However, in recent years, increasing popularity in laboratory research has been gained by hybrid flow batteries in which only one electrode is exposed to the solution of an electroactive compound, while the other electrode is of a different type, *e.g.*, gas diffusion (for example, hydrogen bromine RFB) or solid-phase electrode (for example, zinc bromine RFB), like in a common CPS. This approach

M.M.Petrov. Candidate of Physico-Mathematical Sciences, Assistant at the Laboratory of Electroactive Materials and Chemical Power Sources (EMCPS), MUCTR, Researcher at the Competence Center of the National Technology Initiative (CC NTI), IPCP RAS.
E-mail: mikepetrovm@gmail.com
Current research interests: electrochemical investigations of redox flow batteries, electrochemical and physicochemical investigations of electroactive polymers and films based on them, thermodynamics of electrochemical reactions, microbial fuel cells.
A.D.Modestov. Candidate of Chemical Sciences, Senior Researcher at the IPCE RAS.
E-mail: amodestov@mail.ru
Current research interests: design, fabrication and study of new electrodes, electrocatalysts and membrane electrode assemblies for fuel cells and electrochemical studies of fuel cells based on these materials; study of surface and electrocatalytic phenomena on solid electrodes; development and investigation of hydrogen bromate hybrid redox flow battery
D.V.Konev. Candidate of Chemical Sciences, Senior Researcher at the IPCP RAS.
E-mail: dkfrvzh@gmail.com
Current research interests: preparation and characterization of materials for electrochemical energy sources; development and testing of electrolytes for redox flow batteries; study and description of processes taking place in RFBs; development and fabrication of RFB prototypes; preparation and characterization of electroactive polymers and films based on them.
A.E.Antipov. Doctor of Chemical Sciences, Professor of the MUCTR, Head of the EMCPS Laboratory, MUCTR, Leading Researcher at the IPCE RAS, Chief Researcher at the CC NTI, IPCP RAS, Leading Researcher at the Faculty of Chemistry, Moscow State University.
E-mail: 89636941963antipov@gmail.com
Current research interests: investigation of transport phenomena of electrolyte solutions; theoretical evaluation and modelling of electrochemical processes in redox flow batteries; design and study of high-performance power sources with high specific power and energy characteristics.
P.A.Loktionov. Postgraduate student and engineer at the IPCP RAS, Assistant at the EMCPS Laboratory, MUCTR.
E-mail: paul.loktionov@gmail.com
Current research interests: design and study of redox flow batteries; electrochemical and spectrophotometric studies of redox reactions and electroactive components of RFB electrolytes; design and study of acid–base flow batteries.
R.D.Pichugov. Assistant at the EMCPS Laboratory, MUCTR, Researcher at the CC NTI, IPCP RAS.
E-mail: rompich90@gmail.com
Current research interests: electrochemical investigations of redox flow batteries; electrochemical and physicochemical evaluation of electroactive polymers and films based on them; composite materials based on electroactive polymers and carbon nanomaterials.
N.V.Kartashova. Postgraduate student at the MSU Assistant at the EMCPS Laboratory, MUCTR.
E-mail: kartashova9natali@gmail.com
Current research interests: redox reactions and electroactive electrolyte components of redox flow batteries; electrochemical investigations of halogenate redox couples of hybrid RFBs; electrochemical investigations of hybrid RFBs.
A.T.Glazkov. Assistant at the EMCPS Laboratory, MUCTR, engineer at the IPCP RAS, postgraduate student, Junior Researcher at the IPCE RAS.
E-mail: arteymyshka@gmail.com
Current research interests: electrochemical investigations of redox flow batteries; redox reactions and electroactive components of RFB electrolytes; electrochemical evaluation of electroactive components of RFB electrolytes; development and testing of RFB prototypes and stacks based on them.
L.Z.Abunaeva. Assistant at the EMCPS Laboratory, MUCTR, master's student at the MIPT.
E-mail: abunaeva_lily@mail.ru
Current research interests: electrochemical investigations of redox flow batteries; vanadium redox flow batteries; supercapacitors.
V.N.Andreev. Doctor of Chemical Sciences, Head of the Research Area 'Electrochemistry', Head of the Laboratory of Electrocatalysis of the IPCE RAS.
E-mail: vandr@phyche.ac.ru
Current research interests: study of electroactive polymers; surface and catalytic phenomena on solid electrodes; structure of the electric double layer; electrochemistry of semiconductors and modified electrodes; use of radioisotopes in electrochemical investigations.
M.A.Vorotyntsev. Doctor of Physico-Mathematical Sciences, Professor and Chief Researcher at the IPCE RAS.
E-mail: mivo2010@yandex.com
Current research interests: electrochemistry; electroactive polymers; functional and nanostructured materials; electrochemical energy engineering; mixed conductors; transport phenomena; interfacial physics; chemical kinetic; condensed state physics; electron transfer; biophysics.

Translation: Svitanko Z.P.

preserves the key advantages of RFBs and, at the same time, markedly increases the stored energy density, which currently restricts the further practical implementation of RFBs. Hybrid RFBs are considered in Section 2.2 of the review.

Also, an increasing number of publications are devoted to energy storage systems that, on the one hand, use the key principles of RFBs and, on the other hand, can hardly be classified as hybrid RFBs or, the more so, classic RFBs. Examples are provided by RFBs with semi-solid electrodes, photoelectrochemical RFBs or RFBs using redox mediators. We classified these designs as type II hybrid RFBs and consider them in Section 2.3 of the review.

It should be emphasized that research and development dealing with redox flow batteries are reflected in several comprehensive reviews;[6–19] however, to our knowledge, currently there are no publications that systematically address the position and prospects of RFBs among other energy storage systems and factors stimulating the search for hybrid designs as opposed to classic designs and that compare the features and capabilities of both classic RFBs and various hybrid systems. Without claiming to be exhaustive, the present review is meant to fill this gap.

2. Electric power industry in the general energy consumption structure. Electrochemical power sources

2.1. Evolution of the energy consumption structure and of the role of electricity

During the last decades, the structure of global energy consumption (including transport, heating, *etc.*) has underwent profound, although relatively slow, changes towards increasing percentage of electricity and increasing role of electrochemical energy sources.

Although electricity, as a kind of energy, has been actively used for more than a hundred years, it was long considered to be rather expensive (per unit of consumed energy). One more restricting factor was the impossibility of storing the electrical energy: it was to be consumed as soon as it was generated (just-in-time principle, JIT), and the energy density in the rechargeable power sources (*e.g.*, chemical power sources) was very low compared with hydrocarbon fuels. Therefore, the proportion of electrical energy in the global energy consumption was relatively low, only 18% even in 2010.[1]

The major role in the production of electricity is still played by high-power thermal, nuclear and hydroelectric power plants. This fact leads to several consequences.

First, the number of electrical power plants is moderate; therefore, the generated electricity must be transmitted to consumers located at distances of many hundreds or even (in particular, in Russia) thousands of kilometres, which requires laying of high-voltage power lines over large distances and is associated with high ohmic losses. The task of maintaining the voltage in the consumer network at a constant level stimulated the fabrication of interconnected power grids, at least, at the level of countries.

Second, irregular consumption of electricity brings about the problem of guaranteed generation of electrical energy at a level not lower than the consumption of electricity at any point of time (JIT principle), although the consumed power permanently varies.[20,21] Over periods of several seconds or minutes, the fluctuations are usually insignificant. However, the change in the consumption over 24 h is pronounced: the power consumed during the day is 60 – 100% higher than that at night. The variation of the consumed power over a year is even more pronounced, ranging between the summer peak (related, first of all, to air conditioning systems) and the yearly minimum in spring or in autumn. Meanwhile, large sources of electricity are characterized by long response time, which additionally complicates the solution of the above-indicated problem. It is exceptionally unfavourable, or even impossible, to change the power of these sources of electricity over an interval of several minutes; their efficiency decreases in the case of variable load even over longer periods of time. Apart from the average power, the sources of electricity should also provide an exactly sinusoidal time variation of the current in the consumer network (50 or 60 Hz); furthermore, because of the indicated JIT principle, this balance between the electricity generation and consumption should be ensured at any point in time.

Among energy systems using no hydroelectric energy, high-power steam turbines operating in their most efficient mode were the major producers of electricity (being most economic). An additional contribution was made by steam or gas turbines operating in the hot stand-by mode under low load, being ready to respond to relatively slow variation of electricity consumption. Finally, gas turbine or diesel power generators had to be run in response to quickly varying or peak levels of consumption; these generators were idle for most of time, but could be started in a matter of minutes. Due to the low cost efficiency of these additional power sources, their use considerably increases the cost of electricity during the periods of high consumption, which is reflected in the multiple electricity rates.

In the last decade, it became clear that the further development of power engineering only by increasing the energy consumption without a crucial change in its structure poses a threat for the future of mankind. The production of energy by means of combustion of fossil fuels (thermal power plants, vehicles driven by internal combustion engines, *etc.*) brings about emissions of hazardous compounds (CO, NO_2) and also CO_2, which causes an increase in the average temperature of the Earth's surface, as its concentration in the Earth's atmosphere increases. The development of nuclear power engineering also causes an environmental damage, as it increases accumulation of radioactive waste. Realization of the urgency of this problem coincided in time with a fast decrease in the cost of unit of electricity generated using photovoltaics and wind power (see below). These factors induced an increase in the proportion of electricity in the overall balance of generated energy from 18% in 2010 to 20% in 2018; in the coming decades, it is expected to rapidly grow: up to 29% in 2030 and up to 49% in 2050.[1]

This process is accompanied by a change in the sources of electricity. Among the conventional sources of electricity, only hydroelectric power plants (HPPs) do not poison the environment, but they also cannot be considered environmentally benign due to the necessity to construct a large elevation drop in water bodies, which leads to flooding of large areas. Therefore, other, renewable/alternative sources of electricity started to play the crucial role in the sharp increase in the total electric power production; these electricity sources use the energy that would be otherwise converted to heat: solar radiation, wind, sea tides, biofuel, geothermal springs and so on. Their vigorous development resulted in a fast decrease in the cost of the used devices

and, hence, a decrease in the cost of electricity they generate.

As a result, the proportion of renewable energy sources in the production of electricity, which was 20% in 2010 (of which 76% was generated by HPPs and 18% were produced by wind power stations and photovoltaics), increased to 25% by 2018 (the contribution of HPPs reduced to 50% and the contribution of wind stations and photovoltaics increased to reach 44%). It is expected that the contribution of the renewable energy sources would further increase up to 57% in 2030 and up to 86% in 2050, of which 50 – 60% would be produced by wind power stations and photovoltaics. In advanced countries, the proportions of renewable sources in the generation of electricity are already relatively high: 33% in UK, 40% in Germany and Spain, and 38% in China (2018).[1,22]

However, the straightforward replacement of the conventional sources of electricity by alternative ones is possible only if the proportion of the latter is relatively low. This is due, in particular, to the discrepancy between the distribution over time of day (and also over year) of electricity generation and demand, since the intensity of the former is determined by external factors (sun and wind), which cannot be regulated depending on the needs of the consumer, as it is done in the case of conventional sources (see above). Moreover, the production rate of alternative electric energy sources (even when they are joined into global energy grids) can be predicted only as an average value. However, due to the JIT principle, this is absolutely incompatible with the need to reliably provide the appropriate power at every time point.

The possibility of a sharp and unpredictable drop in the total output of the alternative sources of electricity at any time means that the traditional power grids must constantly have backup power sources (for example, non-environmentally friendly gas turbine or diesel power generators), which would be idle for most of the time and would be turned on only in unfavourable situations.

Consequently, the proportion of the mentioned alternative sources in the total electric power may exceed a certain limit only if they are not directly connected to the consumers of electricity, *i.e.*, if there is an intermediate system capable of rapidly and cost-efficiently converting the electricity generated by sun and wind sources into another kind of energy, which can be converted back to electricity when necessary. Since this temporary energy storage system has been insufficiently developed to date, the periods of acute shortage of electricity for consumers alternate with opposite situations of excess electricity production, resulting in some cases in negative electricity prices.[23,24]

On further increase in the contribution of these, not completely predictable, sources of electrical energy, the total storage capacity of this temporary energy storage system should become sufficiently high as to fully meet — in the case of an unfavourable situation — the demand for electrical energy for the period of time where the primary sources of electricity do not operate for some reason, even if these events are rare. This means that, with increasing proportion of renewable sources of electricity, the amount of energy stored in such systems should gradually become huge (fully covering the demand for electricity for at least many hours). This emphasizes the immensity of the problem of developing the optimal design of these stand-by resources.

Development of energy storage systems would do away with one more problem inherent in conventional energy generation, that is, the need to use very high-power sources of electrical energy, which possess substantial drawbacks (see above). Instead, there appears the possibility of decentralizing the electrical energy sources and fabricating local grids comprising efficient but low-power electricity generation devices on various scales (for single households and larger); this requires the design of economically feasible electricity storage systems of appropriate size.

Balancing between electricity consumption and generation by means of energy storage systems should occur for any time periods ranging from fractions of a second to many hours. Currently, there is no universal energy storage system that would be able to balance the grids over the whole dynamic range, moreover, in the most economically feasible way. For this reason, intensive development of numerous energy storage devices operating on highly diverse principles is in progress.

2.2. Temporary storage of electricity as mechanical energy

2.2.1. Pumped storage hydroelectric power plant (PSHPP)

Like in the case of conventional hydroelectric power plants, electricity is generated by a turbine that is rotated by falling water; however, in this case, water is repeatedly transferred between two water bodies located at different heights. Currently, such devices make the highest contribution (98%) to the total capacity of energy storage systems. Despite a number of benefits (long and cheap operation, high energy efficiency of approximately 80%, quick response speed, *etc.*), they refer to very expensive storage systems because of high capital cost. Furthermore, they can be constructed only in mountainous areas, which contradicts the trend towards decentralization of energy storage systems. Therefore, the percentage of pumped storage hydropower is expected to decrease to 45 – 51% by 2030 at the expense of more rapid development of other types of devices.[2]

2.2.2. Kinetic energy storage

The flywheel and the electric motor that form this electromechanical storage system are usually placed in a sealed vacuum container in which they rotate at 100 000 rpm on mechanical or magnetic non-contact bearings. These devices are compact, environmentally safe and have a long lifetime (more than 20 years); they withstand up to 200 000 charge – discharge cycles and are characterized by high energy efficiency of up to 80 – 90%, low operating costs and the possibility of fast change in the operation mode. Their drawbacks include very high capital cost and high cost of kW h of electricity.[25,26] The major applications are uninterruptible power sources, *e.g.*, used for computer centres. In 2018, they accounted for approximately 0.5% of the total electricity storage capacity;[25] the expected growth is 9% per year.[27]

2.2.3. Pneumatic energy storage

During charging, excess of electrical energy is used for air compression (usually up to 45 – 70 atm.) and pumping to underground cavities. During the discharge, the compressed air from the cavity is directed to gas turbine generators. The efficiency is about 50%. A deeply located leak-proof underground cavity of an appropriate size is required. The ramp-up time is about 15 min.[28] In 2018, they accounted for

approximately 0.24% of the total electricity storage capacity.[25]

2.3. Secondary/rechargeable electrochemical cells

Sources of electricity of various types are used for temporary electricity storage.

2.3.1. Lithium-ion battery

In 2018, this battery accounted for approximately 1% of the total electricity storage capacity; this value has more than tripled in 3 years.[25] They are considered as promising stationary storage systems: the expected growth is almost 1000-fold by 2050.[22] They are characterized by relatively low capital cost,[25] energy density of 250 – 300 W h kg^{-1},[29] energy efficiency of approximately 86%, a large number of charge – discharge cycles, a lifetime of 10 years, low self-discharge and low switch-over time between operation modes.

2.3.2. Sodium sulfur battery

In 2018, this battery accounted for approximately 0.3% of the total electricity storage capacity.[25, 30, 31] This is a high-temperature sealed current source (300 – 350 °C) filled with molten sulfur and sodium separated by a solid oxide electrolyte (β-alumina). The device is characterized by an energy density of ~370 W h L^{-1}, or ~220 W h kg^{-1}, cycle life of up to 4500 charge – discharge cycles, lifetime of up to 15 years, low self-discharge and energy efficiency of approximately 75%. The power density is ~36 W kg^{-1}; the capital cost is high.[25]

2.3.3. Sodium-nickel chloride battery

The difference from the previous case is that a $NaAlCl_4 + NiCl_2$ melt is present at the cathode. The device accounts for less than 0.1% of the total electricity storage capacity.[25, 32]

2.3.4. Lead battery

Despite the wide use, this battery accounts for less than 0.1% of the total electricity storage capacity.[25] The capital and operating costs are relatively low;[25, 33] the switch-over time between the operation modes is fast; nearly 100% disposal of materials after the end of cycle life is possible. The energy density of a lead battery is 35 – 40 W h kg^{-1}, while the power density reaches 180 W kg^{-1}, and the energy efficiency is approximately 70 – 75%. The cycle life of a lead battery is about 1000 charge – discharge cycles; and the average self-discharge intensity is about 40% per year.

2.3.5. Electrochemical (super)capacitor

The device accounts for less than 0.1% of the total electricity storage capacity.[25] It is characterized by a very high power density (up to 6 – 8 kW kg^{-1}) with the energy density being up to 100 – 250 W h kg^{-1}, a very large number of charge – discharge cycles (up to a million), short charge and discharge times, relatively high self-discharge currents, relatively low capital cost with very high cost of unit of electricity.[25] They are used as energy storage devices in uninterruptible power sources to stabilize network parameters over short periods of time, in the transport for regenerative braking systems, often in combination with other storage devices with higher energy storage capacity, but a longer response time, for example, with electrochemical storage systems.[34]

2.3.6. Flow and hybrid batteries

Currently, these devices make a minor contribution to the total energy storage capacity, but they are considered as an upcoming trend of this field. Redox flow batteries (RFBs) are a sort of secondary (rechargeable) chemical power sources. A classical RFB comprises an electrochemical reactor (a set of various MEA called a battery or a stack) and two tanks filled with electrolytes. They convert electrical energy to chemical energy *via* electrochemical reactions of compounds (components of redox couples) dissolved in these electrolytes, with the possibility of recovery of the electrical energy by the same device when necessary depending on the voltage on the contacts.[4]

In the literature, electrolytes used in redox flow batteries are traditionally called catholyte and anolyte, by analogy with other secondary CPS, which is dictated by the direction of electron transfer during the generation of electricity: catholyte is the electrolyte containing oxidant components, while the anolyte contains components of the reductant. In some publications, these terms were replaced by posolyte and negolyte, which is associated with the polarity of electrodes (positive and negative) through which these electrolytes are pumped, irrespective of the direction of the electrode reaction (charging or discharging).

The redox couples are usually systems in which the interconversion occurs as a (quasi)reversible reaction on a relatively inexpensive electrode without electrode modification by expensive catalysts. Numerous redox couples based on iron, vanadium, zinc, chromium, copper, bromine, *etc.* compounds have been studied.[12] As a rule, their solutions have relatively low energy storage capacity, but provide long-term chemical stability, large number of charge – discharge cycles (down to complete discharge) and, owing to their low cost, the possibility of designing large-scale energy storage devices. In addition, these electrolytes do not tend to self-discharge and, therefore, they are advantageous for long-term storage of energy (for more than 6 h intervals).

Classical RFBs have a number of advantages[4] over other CPS types with solid electroactive materials:

(1) independent scalability of the power and capacity, which ensures flexibility of the technology to different-size consumers;

(2) theoretically unlimited lifetime due to the absence of complex distributed hetero-interfaces and phase transitions necessary for the main reaction to proceed;

3) possibility of increasing stack voltage without using balancing circuits between separate elements;

4) absence of self-discharge in the stand-by mode;

(5) the Lenz – Joule heating problem, which is relevant to scaling of lithium-ion storage batteries,[35] is solved due to the fact that RFB electrolyte is simultaneously a heat transfer medium;

(6) the electrolyte cost accounts for a considerable part of the RFB net cost (up to 55%, Ref. 36); however, the electrolyte is barely deteriorated and, after the RFB lifetime is completed, it can be repeatedly used or sold. This increases the economic attractiveness of RFBs.

Out of flow batteries, all-vanadium RFBs based on V^{2+}/V^{3+} and VO^{2+}/VO_2^+ redox couples have been most widely commercialized. However, like other types of classical RFBs, they have low stored energy density, which is a highly important characteristic of distributed energy engineering. Furthermore, classical RFBs are poorly adjusted to discharge – charge pulsed loads and require relatively expensive materials for electrolytes. Therefore, hybrid RFBs that

combine at least some of the above-mentioned benefits of classical RFBs with the benefits of half-cells of other CPS are being actively developed.

Hybrid flow batteries are devices in which electrochemical reactions of different types proceed on the two electrodes. For example, the hydrogen bromine (H_2-Br_2) battery combines the half-reaction $H_2-2e^- = 2H^+$ on the negative electrode (used in fuel cells) and the $Br_2 + 2e^- = 2Br^-$ reaction typical of RFBs on the positive electrode. One more example of a hybrid device is the zinc bromine battery based on the reactions $Zn-2e^- = Zn^{2+}$ and $Br_2 + 2e^- = 2\,Br^-$.[4]

In view of the customary energy consumption structure, which is briefly described above, the practical use imposes a number of requirements to RFBs, which imply the minimization of two major economic parameters, the cost of kW h of electricity and the levelized cost of energy storage. In relation to RFB characteristics, this means that it is necessary to minimize the energy loss of the storage system and increase the discharge power, lifetime and stored energy density. The last-mentioned value is significant for the distributed energy engineering, which means that the storage system should be inserted into a limited space of the surrounding landscape, *e.g.*, urban or industrial one.

Therefore, we will compare various types of RFBs — both implemented in the real economy and occurring at the stage of laboratory research — basing on the following characteristics: power density and the maximum power of the storage system, stored energy density, capacity retention rate upon numerous charge–discharge tests (characterizes the cycle life) and the energy efficiency (characterizes the energy loss of the storage device).

3. Redox flow batteries

3.1. Classical RFBs

3.1.1. All-vanadium RFB

In the beginning of 2020, approximately 40 vanadium redox flow batteries (VRFBs) with a total storage capacity of 37.5 MW were used all over the world as stationary energy storage devices.[37] Six more vanadium storage batteries with a total storage capacity of 210.7 MW were at the design and construction stages, including a large-scale 200 MW/800 MW h complex in the Liaoning province (China).[38] The leading VRFB manufacturers are Dalian Rongke Power Co (China), Prudent Energy (China), Sumitomo Electric Industries (Japan), Uni Energy Technologies (USA), Invinity Energy Systems (USA and UK), STEAG Solar Energy Solutions GmbH (Germany), VRB Energy (Canada, China), Ashlawn Energy (USA), SCHMID Group (Germany). According to analysis,[39] the VRFB market should amount to $625.4 million in 2020, while by the end of 2026, it will reach $6.19 billion. Simultaneously, the cost of VRFB, which was on average $4505 per kW in 2012, decreased to $1916 per kW by 2018.

The possibility of manufacturing redox flow batteries was first mentioned in a patent[40] in which vanadium salts were considered as electroactive electrolytes, together with salts of other metals (Fe, Cr, Co, Ce, Ti, Mn). The first VRFBs were developed by Maria Skyllas-Kazakos' research group at the University of South Wales (Sidney, Australia) in the late 1980s.[41–43]

Figure 1 shows the block diagram of a VRFB. An electrolyte containing vanadium salts in V(IV) and V(V) oxidation states is pumped from tank 1 to the positive

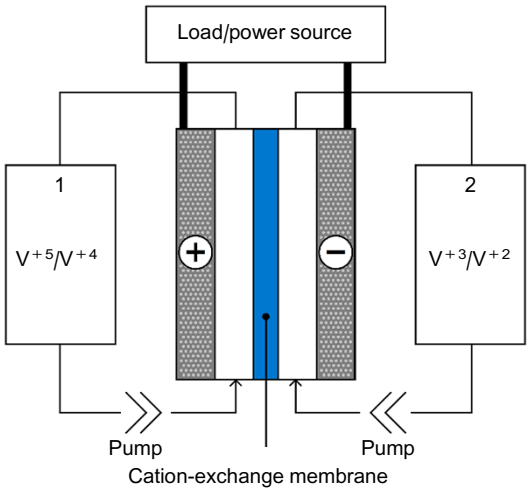


Figure 1. Basic block diagram of vanadium redox flow battery.

electrode compartment of VRFB, while an electrolyte containing V(II) and V(III) salts is pumped from tank 2 to the negative electrode compartment. The redox reactions occur on porous carbon materials, usually, pretreated carbon felt or carbon paper. Electrolytes are circulated through pores of the electrodes pressed to the cation-exchange membrane, which separates the electrode compartments, and then back to the corresponding tanks. Usually, electrolytes in both tanks are dissolved in a 4 M – 5 M aqueous solution of sulfuric acid where vanadium ions are hydrated and exist as $[VO(H_2O)_5]^{2+}$, $[VO_2(H_2O)_4]^+$ and $[V(H_2O)_6]^{2+}$, $[V(H_2O)_6]^{3+}$ ions, respectively.[44]

The following reactions take place on the VRFB electrodes (here and below, the direction from left to right means charging, and the direction from right to left is discharge):

The reaction on the positive electrode:

$$VO^{2+} + H_2O \leftrightarrows VO_2^+ + 2H^+ + e^-;\ E_0 = 1.00\ \text{V (SHE)} \quad (1)$$

The reaction on the negative electrode:

$$V^{3+} + e^- \leftrightarrows V^{2+};\ E_0 = -0.26\ \text{V (SHE)} \quad (2)$$

The overall reaction:

$$VO^{2+} + H_2O + V^{3+} \leftrightarrows VO_2^+ + 2H^+ + V^{2+};\ E_{cell} = 1.26\ \text{V} \quad (3)$$

The difference between the standard potentials of electrode reactions in VRFB is 1.26 V; the open-circuit voltage at the state of charge (SOC) of 50% is approximately 1.4 V, while at 100% SOC, it is 1.6 V. Since the electrodes are made of carbon, the voltage in a single cell during battery charging should not exceed 1.7 V to prevent fast oxidative degradation of the positive electrode. Usually, batteries are operated at SOC values ranging from 5% (fully discharged) to 85% (fully charged),[45] in order to avoid hydrogen evolution on the negative electrode and oxidation of the carbon material of the positive electrode.

The battery charging process is accompanied by the transfer of protons through the cation-exchange membrane from the negative electrode compartment to the positive electrode compartment. Due to high proton transport through the membrane, crossover of vanadium ions is insignificant. The energy density of VRFB is determined by the solubility and stability of vanadium electrolytes, in particular V(V). At 30 °C, solutions of V(V) ions in H_2SO_4 are stable at concentrations below 3 M; however, at 50 °C,

crystals of V_2O_5 precipitate from solutions with concentrations above 1.8 M.[46]

On the other hand, for solutions with V(II), V(III) and V(IV) concentrations at approximately 2 M, lowering the electrolyte temperature below 10 °C results in attainment of limiting solubility in sulfuric acid electrolytes. Thus, the temperature range of VRFB operation and electrolyte storage is limited to 10–40 °C. Correspondingly, the energy density of VRFB with a sulfuric acid electrolyte is limited to 35 W h kg^{-1}. Owing to the high electrical conductivity of the electrolyte, high specific surface area of carbon electrodes and also relatively high rates of electrode reactions, VRFB has a high power density of up to 1.25 W cm^{-2} and higher.[47] Without allowance for auxiliary systems, the energy efficiency of VRFB is 70–90%. Measurements of the electrode potentials of a VRFB cell[48] demonstrated that the exchange current of the carbon paper positive electrode is 44 times higher than that for the negative electrode.

The major benefits of VRFBs are as follows:

(1) the compartments of both electrodes contain only vanadium ions and sulfuric acid; therefore, crossover of ions through the membrane does not result in cross-contamination of electrolytes. This is a very important advantage over RFBs of other types;

(2) in the case of electrolyte imbalance, it is relatively easy to perform the back procedure of balancing;

(3) VRFB withstands up to 100 thousand charge–discharge cycles;

(4) the lifetime of the battery exceeds 10 years.

The major drawback of VRFBs is low energy storage capacity, which is mainly limited by decomposition of $[VO_2(H_2O)_4]^+$ to give insoluble V_2O_5. In the presence of HCl in the catholyte, another vanadium(V) compound, $VO_2Cl(H_2O)_2$, is formed, which is more stable against decomposition to V_2O_5. The addition of phosphoric acid, ammonium sulfate, methanesulfonic acid, potassium hexametaphosphate, urea or some other compounds also stabilizes the catholyte.[44] Mention should also be made of high cost of the starting materials for vanadium electrolytes, which has been steadily increasing in recent years due to high demand for vanadium in metallurgy.

To minimize the capital cost, a lot of studies are carried out to optimize the design of both VRFB stacks and single MEAs. The optimization concerns flow fields for electrolyte delivery, selection of electrode and membrane materials, *etc*. To simplify these studies, Pichugov *et al.*[49] proposed a design of an experimental cell in which all key components of MEA were manufactured from sheet materials by simple technological operations, which allowed easy and fast variation of the MEA composition. The robustness of this concept on scaling was also confirmed[50] in relation to a VRFB stack comprising ten MEAs.

3.1.2. Iron chromium RFB

The idea of iron chromium RFB was independently proposed in the 1970s–1980s in the USA (NASA) and in Japan (Mitsui).[51–53] The Fe^{2+}/Fe^{3+} redox couple (*e.g.*, $FeCl_3$/-$FeCl_2$ salt) is used as the catholyte, and the Cr^{2+}/Cr^{3+} redox couple (*e.g.*, $CrCl_2/CrCl_3$ salt) serves as the anolyte; see Eqns (4)–(6). Most often, hydrochloric acid serves as the supporting electrolyte, and the positive and negative electrode half-cells are separated by a proton exchange membrane.

The reaction on the positive electrode:

$$Fe^{2+} \leftrightarrows Fe^{3+} + e^-;\ E_0 = 0.77\ \text{V (SHE)} \quad (4)$$

The reaction on the negative electrode:

$$Cr^{3+} + e^- \leftrightarrows Cr^{2+};\ E_0 = -0.41\ \text{V (SHE)} \quad (5)$$

The overall reaction

$$Fe^{2+} + Cr^{3+} \leftrightarrows Fe^{3+} + Cr^{2+};\ E_{cell} = 1.18\ \text{V} \quad (6)$$

The lowest solubility among the electrolytes used in iron chromium RFB is inherent in $CrCl_3$ (2.2 M); hence, the theoretical stored energy density does not exceed 70 W h L^{-1} of the anolyte. The power density of the best laboratory prototypes of iron chromium RFB reaches 1080 mW cm^{-2} at elevated temperature (65 °C) and 700 mW cm^{-2} at room temperature (25 °C).[54] The energy efficiency ranges from 70 to 85%, depending on the cell used, electrolyte composition, charge–discharge cycling conditions and temperature, and can reach 88%.[55]

In comparison with VRFB, an iron chromium battery has advantages of low cost ($17 per kW h of electricity) and low toxicity of the used electrolytes.[56] However, iron chromium RFBs also have some drawbacks:

— the Cr^{2+}/Cr^{3+} redox transition is slow. The rate constant for the electron transfer for the Fe^{2+}/Fe^{3+} couple amounts to 8.6×10^{-2} cm s^{-1} (when heat-treated carbon materials are used as electrodes),[57] whereas for the Cr^{2+}/Cr^3 couple, this rate constant does not exceed 1.35×10^{-3} cm s^{-1}.[58] This brings about the necessity of using catalysts, most often, based on bismuth, on the anode. Meanwhile, these compounds can be oxidized with air or iron ions, and their presence may have an adverse effect on the electrode and membrane performance during long-term RFB operation.

The used electrolytes are unstable at room temperature; therefore, for stable operation of RFB it is necessary to maintain the temperature of electrolytes at about 65 °C or restrict the potential range of charge–discharge cycling, which leads to decreasing accessible capacity of the storage system.

Nevertheless, iron chromium RFBs remain among the few types of RFBs used in real applications. In 2015, EnerVault company commissioned an energy storage system combining iron chromium RFBs and photovoltaic cells with a maximum power of 250 kW and a capacity of 1 MW h. According to testing results, the system successfully provided consumers with alternating current at a power of 250 kW for 4 h.[59]

3.1.3. Polysulfide halide RFB

The idea of polysulfide bromide RFB was proposed in 1983.[60] Aqueous alkaline solutions of sodium bromide (NaBr) and sodium polysulfide (Na_2S_x) are used as the catholyte and anolyte, respectively.[61] The cathode redox couple is Br_2/Br^{-1} and S_{x+1}^{2-}/S_x^{2-} is the anode redox couple. Apart from Br^- and Br_2, the complex compound of Br_3^- is formed in the catholyte, while in the anolyte, elemental sulfur can form di-, tri- or tetrasulfide anions. The positive and negative half-cells are separated by a membrane permeable for Na^+ ions. The reactions occurring in polysulfide bromide RFBs are described by Eqns (7)–(9).

The reaction on the positive electrode

$$2\,NaBr \leftrightarrows 2e^- + Br_2 + 2Na^+;\ E_0 = -0.27\ \text{V} \quad (7)$$

The reaction on the negative electrode

$$2Na^+ + (x-1)\,Na_2S_x + 2e^{-1} \leftrightarrows x\,Na_2S_{x-1}; \quad (8)$$

$$x = 2\text{–}4,\ E_0 = -1.06\ \text{V}$$

The overall reaction

$$2\,NaBr + (x-1)\,Na_2S_x \leftrightarrows Br_2 + x\,Na_2S_{(x-1)}; \quad (9)$$
$$E_{cell} = -1.33\ V$$

As compared with many other RFBs, polysulfide bromide batteries use less expensive electrolyte components, but they also suffer from some drawbacks:

— ohmic resistance of the cation-exchange membrane in the Na^+ form is substantially higher than that for the membrane in the H^+ form. This markedly decreases the power density and the energy efficiency of the system and simultaneously precludes the use of high current densities, which narrows down the scope of applicability of these RFBs. For example, even at the current density of 40 mA cm^{-2}, the typical energy efficiency does not exceed 80%;

— the S_{x+1}^{2-}/S_x^{2-} redox transition is characterized by retarded electron transfer. This necessitates the deposition of cobalt- or nickel-based catalysts on the electrodes made of carbon materials, which substantially increases the cost of the system;

— redox reactions are accompanied by side reactions, first of all, precipitation of elemental sulfur, which leads to capacity loss and increases the cell resistance;

— the presence of toxic and corrosive bromine compounds considerably reduces the operational safety and serves as the key factor of degradation of the electrodes of energy storage devices based on polysulfide bromide RFBs.

The last-mentioned problem can be solved by replacing the bromine/bromide redox couple by other halides. For example, Li *et al.*[62] used the I_3^-/I^- redox couple, in combination with the S_2^{2-}/S^{2-} couple on the cathode, and the half-reactions were balanced due to the transport of K^+ cations through the membrane.

The theoretical energy density in this system reaches 85.4 W h L^{-1}, while the real value was 49.4 W h L^{-1}, with the specific discharge capacity being 52.9 A h L^{-1} (a 6 M KI solution as the anolyte and a 3.3 M K_2S_2 solution as the catholyte). The current density during charge – discharge cycling was 20 mA cm^{-2} and the electrolyte flow rate was 4 mL min^{-1}. The coulombic efficiency varied from 86 to 93% (depending on the electrolyte composition), the voltaic efficiency ranged from 73 to 78%, and the energy efficiency was from 63 to 73%. Low values of coulombic efficiency were attributed to side reactions that took place upon cross-mixing of electrolyte components of both half-cells.

The use of redox couples based on other halogens does not eliminate many of the mentioned typical problems of polysulfide bromide RFBs: high ohmic resistance of membranes in the Na^+ or K^+ form, the necessity of using expensive catalysts as parts of anodes. Although there are known cases of using energy storage devices based on polysulfide bromide RFBs with an energy storage capacity of up to 15 MW h (Regenesys Ltd., UK),[63] further expansion of this technology is now open to question.

3.1.4. Anthraquinone bromine RFBs

The first anthraquinone bromine RFB (ABRFB) was reported in 2014 by Professor Michael J. Aziz's research group (Harward).[64] They used an 1 M sulfuric acid solution of 9,10-anthraquinone-2,7-disulfonic acid AQDS (structure **1**) as the anolyte and the 3 M HBr + 0.5 M Br_2 mixture as the catholyte. Nafion 212 and 115 ion-exchange membranes were used as separators; the half-reactions were balanced by means of H^+ transport. The chemical reactions taking place in ABRFB are described by Eqns (10) – (12).

The reaction on the positive electrode

$$3\,Br^- \leftrightarrows Br_3^- + 2\,e^-;\ E_0 = 1.05\ V \quad (10)$$

The reaction on the negative electrode

$$AQDS + 2\,e^- + 2\,H^+ \leftrightarrows AQDSH_2;\ E_0 = 0.22\ V \quad (11)$$

The overall reaction

$$AQDS + 2\,H^+ + 3\,Br^- \leftrightarrows AQDSH_2 + Br_3^-;\ E_{cell} = 0.83\ V \quad (12)$$

The theoretical stored energy density of this battery reaches 50 W h L^{-1}. At 90% SOC, the tested cell showed an average open-circuit voltage of 0.92 V and a power density of 0.6 W cm^{-2}. According to the results of 15 charge – discharge cycles with a current density of 200 mA cm^{-2}, the coulombic efficiency was 95%, while for the current density of 500 mA cm^{-2}, the electrolyte capacity retention was ~99.2% for each cycle.

This type of RFB offers a number of key advantages over the most popular VRFBs:

— ABRFB electrolytes can be fabricated from cheap and readily accessible starting materials. According to estimates as of 2014,[64] the unit cost of the feedstock for ABRFB electrolytes is approximately \$27/kW h, while for VRFB this value reaches \$81/kW h;

— the AQDS/$AQDSH_2$ couple experiences a two-electron redox transition proceeding at a high rate (according to updated data, in acid media, a 1.5-electron transition takes place[65]);

— anthraquinone derivatives are virtually not prone to crossover through semipermeable polymer membranes;

— AQDS has higher solubility in aqueous acidic solutions (up to 1 M) than many other quinones.

However, the proposed batteries suffer from several drawbacks. The key drawbacks are as follows:

— toxicity and corrosivity of molecular bromine;

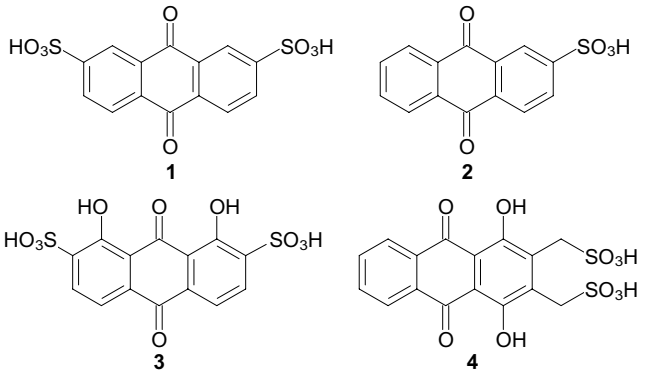
— high viscosity of AQDS solutions (with concentrations of > 0.1 – 0.2 M) at room temperature, which results either in increasing energy expenditure for electrolyte pumping or in the necessity of maintaining high temperature of the anolyte;

— the crossover of molecular bromine from the cathode to anode half-cell leads to rather fast decay of ABRFB storage capacity during multiple charge – discharge cycling due to side chemical reactions between bromine compounds and anthraquinone derivatives.

A series of subsequent studies, performed by Aziz's group and other research groups, outlined some ways of overcoming these difficulties. For example, Azis and coworkers[66,67] optimized the composition of bromine-containing catholyte, modified the electrodes, with all cycling being conducted at an elevated temperature (40 °C). This increased the power density up to 1.6 W cm^{-2} and increased the capacity utilization rate and energy efficiency: for cyclic charge – discharge cycling at a current density of 100 mA cm^{-2}, these values were 95 and 80%, respectively.

Gerhardt *et al.*[68] explored the possibility of replacing AQDS by other anthraquinone-derived sulfonic acids (structures **2** – **4**). Dihydroxylated derivative **3** is even more prone to undergo side reactions with bromine compounds than AQDS. One more derivative, namely, 1,4-dihydroanthraquinone-2,3-dimethylsulfonic acid **4**, proved to be unsuitable due to irreversibility of most redox reactions. Meanwhile, RFBs using sulfuric acid solutions of anthra-

Structures 1 – 4



quinonesulfonic acid AQS (**2**) as the anolyte were even superior, in some characteristics, to AQDS-based batteries. The use of such RFBs increased the power density (700 mW cm^{-2} for AQS *versus* 600 mW cm^{-2} for AQDS; 90% SOC) and the energy efficiency (73.5 and 62% for AQS- and AQDS-based cells, respectively). These changes were attributed, first of all, to the higher standard redox potential E_0 of the $AQSH_2$/AQS couple compared to the $AQDSH_2$/AQDS couple and, as a consequence, the higher open-circuit voltage of the cell. However, the capacity retention rate remained virtually invariable (being ~99% per cycle).

Finally, Khataee *et al.*[69] proposed an RFB concept in which the anodic and cathodic half-reactions occurred at different pH: a 0.5 M solution of Na_2AQDS in 2 M NH_4Br (pH 8) served as the anolyte and a 2 M solution of NH_4Br/0.3 M Br_2 (pH 2) was used as the catholyte. As a result, the standard cell potential increased to 1.3 V, the average capacity utilization rate determined after 200 charge – discharge cycles was 93%, the charging capacity was 1.81 A h, and the capacity retention rate (the average value per cycle) was 99.98%.

However, the ABRFB concept still remains at the level of laboratory prototypes both due to the difficulties described above (considerable loss of capacity caused by bromine crossover and corrosivity and toxicity of bromine) and due to the fact that the practical possibility of using anthraquinone-containing electrolytes obtained from inexpensive and readily accessible starting materials (*e.g.*, by sulfonation of anthraquinone with oleum) has not yet been demonstrated.

3.1.5. Miscellaneous organic RFBs

The use of organic electrolytes in RFBs opens up broad prospects for two main reasons. First, the starting materials used to prepare them are cheaper than salts of some metals such as vanadium. Second, there is an enormous diversity of organic electrolytes and options for chemical structure modification. The use of various anthraquinonesulfonic acids as RFB anolytes is described above. Below we briefly illustrate other examples involving some electroactive organic compounds typically used in RFBs such as quinones, viologens (quaternary dipyridyl salts), (2,2,6,6-tetramethylpiperidin-1-yl)oxyl TEMPO (**12**) derivatives and electroactive polymers.

Electrolytes based on quinones. Historically, quinones are among the first organic electroactive compounds to be used as RFB electrolytes because of a high rate of redox transitions. Yang *et al.*[70] used a 0.5 M solution of 2,5-dihydroxy-1,4-benzoquinone DHBQ (structure **5**) in 2 M KOH as the anolyte, while a 0.4 M solution of potassium hexacyanoferrate(II) $K_4[Fe(CN)_6]$ in 1 M KOH served as the catholyte. Nafion polymer membranes were used as separators; the reactions taking place in the cell are represented by Eqns (13) – (15).

The reaction on the positive electrode

$$Fe(CN)_6^{4-} \leftrightarrows Fe(CN)_6^{3-} + e^-;\ E_0 = 0.51\ V\ (pH\ 14) \quad (13)$$

The reaction on the negative electrode

$$DHBQ + 2e^- + 2H^+ \leftrightarrows DHBQH_2;\ E_0 = -0.72\ V\ (pH\ 14) \quad (14)$$

The overall reaction

$$DHBQ + 2Fe(CN)_6^{4-} + 2H^+ \leftrightarrows DHBQH_2 + 2Fe(CN)_6^{3-};\ E_{cell} = 1.21\ V \quad (15)$$

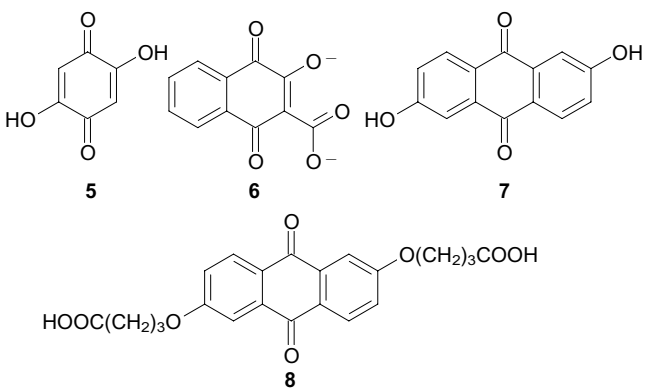
The open-circuit voltage of this cell for 100% SOC amounted to 1.25 V, and the peak power density was 300 mW cm^{-2}. During the charge – discharge cycling with a current density of 100 mA cm^{-2}, the coulombic efficiency in the first cycle was 77% and the specific capacity was 23.15 A h L^{-1}, which corresponded to a capacity utilization rate of 91.8%. After 10 cycles, the coulombic efficiency decreased to 72%, while the capacity utilization rate was as low as 86.4%. Low coulombic efficiency and fast drop of the capacity were dictated by two principal factors, that is, crossover of DHBQ molecules through the membrane and high susceptibility of quinones to side reactions, first of all, nucleophilic substitution reactions.

Wang *et al.*[71] used a bulkier molecule, 2-hydroxy-3-carboxynaphthoquinone **6** (0.5 M HCNQ in 1 M KOH, pH 14), in combination with the same catholyte. This decreased the crossover impact and, hence, increased the stability of the system: at the end of 100 charge – discharge cycles at a current density of 100 mA cm^{-2}, the overall capacity retention rate was 94.7%.

Finally, the crossover was further suppressed on going from quinones to bulkier anthraquinone derivatives. With 2,6-hydroxyanthraquinone **7** being used as the catholyte, the capacity retention rate reached 99.9% (100 charge – discharge cycles at a current density of 100 mA cm^{-2}; the value was calculated per cycle),[72] while in the case of catholyte **8**, this value increased to 99.999%, which is comparable with the best VRFB designs.[73]

One more considerable drawback of quinone-based RFB electrolytes is their sparing solubility (especially in aqueous acidic solutions), which dictates relatively low RFB energy densities. For example, in the study of Kwabi

Structures 5 – 8



et al.,[73] this value did not exceed 17 W h L^{-1}, since the maximum solubility of **8** in 1.2 M KOH is 1 M; furthermore, the concentration of only 0.1 M was tested in the study.

Electrolytes based on viologens and TEMPO. Viologen-based electroactive compounds represent one more widely used group of organic anolytes. A typical example was reported by Liu *et al.*,[74] who used a 1 M solution of methyl viologen MV (**9**) in 1 M aqueous NaCl solution as the anolyte and hydroxylated TEMPO (**13**) (0.5 M in 1 M aqueous NaCl) as the catholyte, with the half-reactions being balanced by the transfer of Cl^- ions through the anion-exchange membrane. The occurring reactions are described by Eqns (16) – (18).

The reaction on the positive electrode

$$TEMPO^{\bullet} \leftrightarrows TEMPO^+ + e^-;\ E_0 = 0.80\ V \quad (16)$$

The reaction on the negative electrode

$$MV^{2+} + e^- \leftrightarrows MV^{\bullet+};\ E_0 = -0.45\ V \quad (17)$$

The overall reaction

$$TEMPO^{\bullet} + MV^{2+} \leftrightarrows TEMPO^+ + MV^{\bullet+};\ E_{cell} = 1.25\ V \quad (18)$$

The MV solubility in water can reach 2.1 M; however, the maximum concentration of solutions used in the study was 0.5 M. After 100 charge – discharge cycles at a current density of 60 mA cm^{-2}, the voltaic efficiency and energy efficiency were 63% and 62%, respectively, the capacity retention was 89%, and the theoretical stored energy density was estimated as 8.4 W h L^{-1}. These relatively low values are attributable to two key drawbacks of viologens regarding their use in RFBs: first, the two-electron reduction of many viologens (in particular, MV) is largely irreversible and, therefore, the charge – discharge of these RFBs is limited to a single-electron reaction. Second, viologens in the partially reduced radical cation form tend to undergo side reactions (oxidation with oxygen and dimerization), which markedly decreases the RFB capacity on prolonged use.

However, the numerous ways of changing the chemical structure of the viologens make it possible to eliminate these drawbacks. For example, modification of the MV molecule with alkyl groups bearing two additional quaternary nitrogen atoms at the ends (BTMAP-Vi, **10**) markedly decreases the proneness of reduced viologen molecules to dimerization due to increasing role of Coulomb interactions between molecules. As a result, RFB performance is improved:[75] for a cell using a 1.3 M solution of BTMAP-Vi chloride as the anolyte and a 2 M solution of ferrocene derivative **15** as the catholyte, the capacity retention rate was 98.58% after 250 charge – discharge cycles. In this case, only single-electron redox transformations of viologens were used in RFB operation.

In another study,[76] apart from introduction of two quaternary nitrogen atoms, the viologen structure was additionally modified in such a way that the pyridine rings were separated by thiazolo[5,4-d]thiazole (**11**). This modification not only increased the chemical stability of the molecule in comparison with MV, but also allowed the use of two-electron redox transitions, because the redox reaction became much more reversible. TEMPO derivative **14** served as the catholyte.

The highest water solubility of the described viologen was 1.3 M, and the standard potential of the cell was 1.44 V. For two-electron transfer, this corresponds to theoretical energy density of 53.7 W h L^{-1}, which is already much higher than the corresponding value for VRFBs. However, in practice, the concentration of viologen did not exceed 0.1 M.

Also, viologens can be used to develop symmetric RFB electrolytes; for example, the $[(bpy\text{-}(CH_2)_3NMe_3]^{2+}\,2\,I^-$ salt served simultaneously as the redox-active component of the anolyte and catholyte and as the supporting electrolyte.[77] This RFB demonstrated an energy efficiency of about 99.5% over 100 charge – discharge cycles at a current density of 10 mA cm^{-2}.

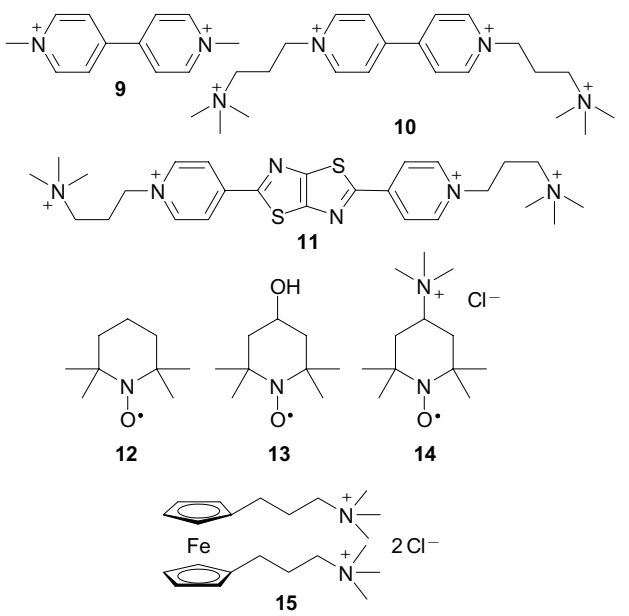
In RFBs using viologen derivatives as anolytes, catholytes are often represented by TEMPO-based compounds. Apart from the common benefits (readily available feedstock; high rate of redox transitions), they are also less prone to side reactions than other electroactive organic compounds. The main drawback of TEMPO is low solubility, which is increased upon various modifications of the molecular structure.

For example, the introduction of trimethylammonium as a side substituent into the TEMPO molecule (**14**) increased its water solubility to 3.2 M.[78] In practice, a 2 M solution of **14** in 1 M aqueous NaCl was used as the catholyte, a 2 M solution of MV with the same aqueous supporting electrolyte served as the anolyte, and an anion-exchange membrane was employed as the separator. The standard potential of the cell was 1.4 V, which corresponds to the theoretical energy density of 54 W h L^{-1} (for the highest solubility; the energy density of 38 W h L^{-1} was demonstrated in the study). When 100 charge – discharge cycles at a current density of 80 mA cm^{-2} were carried out, the overall capacity retention rate was almost 100%.

In addition, TEMPO and its derivatives can also be used with anolytes other than viologens. Such examples are mentioned in the following Sections.

Electrolytes based on electroactive polymers. Due to a large size of macromolecules, polymeric organic RFBs have an important advantage over other types of RFB: they do not require expensive ion selective membranes, since less expensive membranes are applicable. In addition, electro-

Structures 9 – 15



active polymers are often more stable during charge–discharge cycling than low-molecular-weight compounds, because steric restrictions occurring in macromolecules decrease their reactivity, and electroactive polymers are less prone to undergo side reactions.[13] However, many electroactive polymers are sparingly soluble (especially in aqueous solutions), which makes the stored energy density of RFBs with these polymers very low. Therefore, the search for alternative designs is in progress: for example, true solutions of polymers are replaced by colloidal systems (see Section 2.3.1).

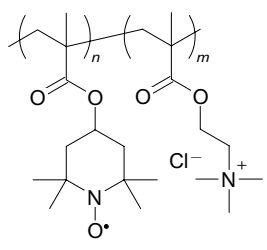
One more alternative is the use of macromolecules with complex architecture. For example, in a study of Janoschka *et al.*,[79] the TEMPO and viologen electroactive groups were moved to side chains, and the backbones were represented by polystyrene and poly(methyl methacrylate) decorated with cationogenic groups to increase the solubility. A solution of polystyrene with a bipyridine group (**17**) was used as the anolyte, a solution of poly(methyl methacrylate) with a TEMPO side group (**16**) was employed as the catholyte, aqueous NaCl solution was the supporting electrolyte, and a cellulose-based dialysis membrane was used as the separator.

The stored energy density for this cell was 8 W h L^{-1}, while the capacity utilization rate for charge–discharge cycling at a current density of 40 mA cm^{-2} was 75%. Furthermore, RFBs demonstrated relatively high stability: the overall capacity retention after 10 000 charge and discharge cycles at a current density of 20 mA cm^{-2} was 80%.

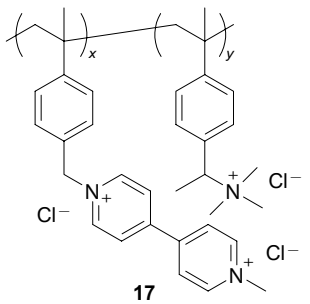
Thus, organic RFBs possess important benefits: organic electrolytes can be obtained from readily accessible and cheap starting materials, and redox reactions are characterized by a high rate of electron transfer and do not require additional expensive catalysts. Meanwhile, the applicability of organic electrolytes in RFBs is strongly restricted by their relatively low solubility (especially in aqueous media) and susceptibility to side reactions. These adverse factors can be minimized by varying the chemical structure of organic molecules, which is often successful; however, currently, there are no industrial prototypes of RFBs operating on organic compounds.

Other types of classic RFBs described above and operating with inorganic electrolytes are much better developed and, hence, commercialized. First of all, this refers to VRFBs. Owing to their unique advantages over other types of CPS with solid electroactive materials (independent scalability of the power and capacity characteristics of the system; absence of self-discharge; theoretically unlimited lifetime, *etc.*), they are already used as stationary energy storage devices with a capacity of up to 800 MW h.[38]

Structures 16, 17



16



17

3.2. Hybrid RFBs, type I

Hybrid RFBs combine the benefits of the classic RFBs with the benefits of other CPS half-cells. Active research and development in this field are stimulated by (i) relatively low stored energy density of classic RFBs and moderate power density, which restrict the possibility of operating with pulses or short-term surges of rated charge and discharge currents and (ii) the desire to lower the capital cost by using less expensive materials, increasing the energy efficiency and lifetime of the system, *etc.*

3.2.1. Zinc bromine RFB

A zinc bromine battery is a typical hybrid RFB. Redox reactions involving bromine species and bromide ions dissolved in aqueous electrolyte take place on the flow positive electrode, while zinc electrodeposition/dissolution takes place on a negative electrode.

The concept of zinc bromine battery was proposed back in 1885,[80] however the design of that current source did not imply electrolyte circulation. Liquid bromine formed on the carbon electrode upon electrolysis of an aqueous solution of $ZnBr_2$ during charging was accumulated on the bottom of the vessel. This idea was not further developed because of fast self-discharge caused by high solubility of bromine in the electrolyte and, hence, fast corrosion of the zinc electrode. The situation was aggravated by the formation of dendrites upon zinc deposition, which resulted in short-circuiting of electrodes.

In the 1970s, Exxon[81] and General Electric attempted to develop a competitive flow battery of this type. Later, the ZBB Corp (Australia) designed a modular energy storage device with a megawatt power level, but several years ago they had to shut down these studies.[82] Currently, commercial storage devices of this type are manufactured by Redflow (Australia) and Primus Power (USA).[83] The total power of the operating storage systems of this type by the beginning of 2020 was 4.25 MW, two more projects on the development of storage systems with a total power of 25.1 MW were at the design and construction stage.[84] According to one of these projects, it is planned to construct in Kazakhstan a set of energy storage devices comprising 1250 RFBs with a total power/capacity of 25 MW/100 MW h. The goal of this project is to increase the proportion of renewable energy sources in the production of electricity in Kazakhstan to 30% in 2030 and to 50% in 2050. Commercial storage systems based on zinc bromine batteries have energy and power densities of 42 W h kg^{-1} and 21 W kg^{-1},[83] with the theoretical material energy capacity being 440 W h kg^{-1}.[85] The energy efficiency for this storage system is approximately 70%,[84] while the capital cost is about $1500 per kW h.[37] The battery capacity provides 2–5 h of discharge at the rated power.[82,83] The calendar lifetime of the energy storage device is 20 years with several thousand charge–discharge cycles. The operating temperature of the battery is 15–50 °C.

Zinc has been widely used in current sources for more than 150 years as a cheap electrode material with high electrochemical equivalent of 820 A h kg^{-1} and a high negative equilibrium potential. According to the Pourbaix diagram,[86] the zinc potential is more negative than the equilibrium hydrogen potential over the whole pH range of aqueous solutions. The stability of zinc is determined by the region of high hydrogen overpotential. In the pH range of 0–8 at room temperature, the equilibrium potential of zinc does not depend on pH and equals

$$E = -0.763 + 0.0295 \log[Zn^{2+}] \text{ (SHE)} \quad (19)$$

The following reactions occur on the electrodes of a zinc bromine flow battery:

The reactions on the positive electrode

$$2\,Br^- \leftrightarrows Br_2 + 2\,e;\ E_0 = 1.087 \text{ V (SHE)} \quad (20)$$

The reactions on the negative electrode

$$Zn^{2+} + 2e \leftrightarrows Zn;\ E_0 = -0.76 \text{ V (SHE)} \quad (21)$$

The overall reaction

$$ZnBr_2 \leftrightarrows Zn + Br_2;\ E_{cell} = 1.85 \text{ V} \quad (22)$$

The electrolyte pH in a zinc bromine redox flow battery is maintained in the range from 1 to 3. This range is determined by the zinc stability region in aqueous solutions, on the one hand (pH > 1), and by formation of bromate upon disproportionation of bromine (pH > 3),[86] on the other hand. The overpotential of hydrogen evolution on zinc is very high; therefore, when the battery is charged, zinc is deposited on the negative electrode with almost 100% current efficiency, whereas zinc corrosion with hydrogen evolution from water virtually does not take place.

The electrode compartments are usually separated by a cation permeable membrane or a porous diaphragm, which prevents the transport of dissolved bromine from the positive electrode compartment to the zinc negative electrode. An aqueous solution of $ZnBr_2$ serves as the electrolyte in both flow circuits. During discharge of the battery, the $ZnBr_2$ concentration increases to ~3 M, while as the battery is charged, the concentration decreases to ~1 M. The diagram of the battery is depicted in Fig. 2.

The negative electrode is made of zinc metal electrochemically deposited on a carbon–polymer composite or titanium substrate. The positive electrode consists of carbon–polymer composite or titanium with a ruthenium titanium oxide coating.[81] The electrolyte circulation through the negative electrode compartment makes it possible to produce relatively thick zinc layers without dendrite growth during charging. The capacity of the battery is determined by the amount of zinc deposited on the negative electrode during charging, being up to 0.15 A h cm^{-2}. The battery is mainly manufactured using polymer and carbon–polymer composites. This is due to high chemical reactivity and corrosivity of bromine-containing electrolytes and to prevention of the deposition of metals with low hydrogen overpotential on the negative electrode.

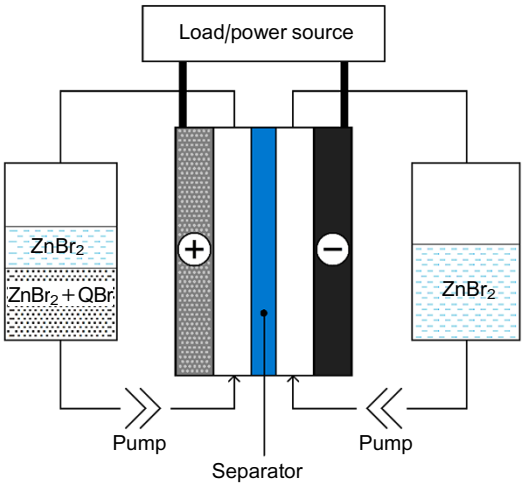


Figure 2. Basic diagram of zinc bromine RFB.

In water, zinc bromide is ionized. The dissolved molecular bromine and bromide ions form Br_3^-, Br_5^- and Br_7^- complexes; as a result, the Br_2 concentration in the electrolyte decreases; hence, bromine vapour pressure also decreases. At the battery operating temperature, bromine is a liquid with a density of 3.1 g cm^{-3}, the boiling point of 58.8 °C, and a high vapour pressure. Bromine vapour corresponds to hazard class 2; the maximum allowable concentration of bromine vapour in the workplace air is 0.5 mg m^{-3},[87] therefore, organic compounds that form complexes with bromine are used to decrease the Br_2 concentration in the electrolyte and prevent the formation of bromine liquid phase.[88] These compounds designated in Fig. 2 as QBr are located on the bottom of the tank in the positive electrode circuit, with $ZnBr_2$/QBr ratio being ~3/1. Symmetrical and unsymmetrical tetraalkylammonium bromides are usually employed for reversible binding of bromine. These compounds reversibly bind bromine to form complexes. As a result of complex formation, the concentration of molecular bromine in the electrolyte of a charged battery decreases to ~0.1 M, which is lower than bromine solubility in the electrolyte. Correspondingly, the bromine vapour pressure above the electrolyte also decreases.

Apart from the above-mentioned benefits of RFBs, one more advantage of zinc bromine batteries is that they are fabricated using cheap reactants and materials (zinc, carbon–polymer composites, separator).

A drawback of this type of redox battery is that the use of zinc electrode precludes the possibility of independent variation of the power and the stored energy, as the thickness of the zinc layer on the electrode cannot exceed a certain limit, which is dictated by the formation of dendrites.[89] One more drawback is the possibility of hydrogen evolution on the zinc electrode during charging of the battery caused by deposition of impurity metals with low hydrogen overpotential. The evolution of hydrogen leads to a decrease in the energy efficiency of the battery and violation of the mass balance between the electrolytes of the positive and negative electrodes.

3.2.2. Other RFBs with zinc metal anode

A zinc metal anode provides high values of theoretical stored energy density; therefore, attempts are made to combine this anode with other redox couples. Winsberg *et al.*[90] utilized solutions of polymers with TEMPO functional groups in side chains as catholytes. Four catholyte compositions were tested, two aqueous and two nonaqueous ones. The best characteristics were found for the anolyte based on the P1 polymer dissolved in a mixture of dimethyl, diethyl and ethylene carbonates in the presence of the 0.75 M $Zn(ClO_4)_2 \cdot 6\,H_2O$ supporting electrolyte. The standard potential of the cell was 1.7 V, the open-circuit voltage at 50% SOC was 1.69 V and the theoretical stored energy density was 8.1 W h L^{-1}. After 500 charge–discharge cycles with a current density from 0.5 to 4.0 mA cm^{-2}, the average capacity retention rate (per cycle) was 99.96%. Upon transition to aqueous electrolytes (an aqueous solution of P2 polymer in the 1 M $ZnCl_2$ + 1 M NH_4Cl supporting electrolyte served as the catholyte; the anode half-cell was filled with 1 M $ZnCl_2$), the stored energy density decreased to 4.1 W h L^{-1}.

This cell is one of the first RFBs with organic redox couples in aqueous electrolytes able to operate at voltages close to 2 V. This was possible due to a relatively high negative E_0 value of the Zn/Zn^{2+} redox couple (−0.76 V *versus* SHE) and considerable overpotential of hydrogen evolution on the anode made of zinc metal, which made it possible to enter the regions inaccessible for, *e.g.*, electrodes based on carbon materials without additional energy loss. The half-reactions were balanced by the transport of Zn^{2+} cations through a regenerated cellulose membrane; this transport is much more difficult than, for example, proton transport through semi-permeable Nafion membranes. As a result, the current density in such a system is markedly limited, being not higher than several tens of mA cm^{-2} for aqueous electrolytes and not higher than 5 mA cm^{-2} for nonaqueous electrolytes. This considerably decreases the applicability of this system for solving practical problems of energy storage. In addition, long-term charge–discharge cycling of this cell induces the growth of zinc metal dendrites, which further restricts the functionality of the system.

Li *et al.*[91] also used the Zn/Zn^{2+} redox couple in the anode half-reaction, but with carbon felt rather than zinc metal as the anode. Identical ZnI_2 solutions served as the anolyte and the catholyte. The half-reactions were balanced *via* the Zn^{2+} transport across the Nafion 115 membrane.

The theoretical stored energy density in a zinc polyiodide RFB is estimated as 322 W h L^{-1} (with the maximum ZnI_2 solubility being 7 M); at the 5 M concentration used in the study, the energy density was 166.7 W h L^{-1}. The average discharge voltage varied from 0.96 to 1.26 V depending on the concentration of the electroactive compound. As a result of 40 charge–discharge cycles at a current density from 5 to 20 mA cm^{-2}, the coulombic efficiency varied from 99.5 to 96.3% (in 0.5 M and 5 M ZnI_2 solutions, respectively), the voltaic efficiency ranged from 91.3 to 70.4%, and the energy efficiency was from 90.9 to 67.8%. The capacity retention rate was >99% per cycle. It was also demonstrated that the addition of ethanol suppressed the growth of zinc dendrites on the anode surface.

Thus, the zinc polyiodide RFB has a high stored energy density even in aqueous electrolytes, while the replacement of the bromine/bromide redox couple by a iodine/iodide couple eliminates the problem of corrosion resistance of electrodes and toxicity of electrolytes. However, relatively low current densities used in charge–discharge cycling due to low mobility of Zn^{2+} ions in the membranes are still a significant problem for this type of battery.

3.2.3. Lithium redox flow battery

The concept of lithium flow battery combines the advantages of lithium-ion batteries and RFBs. When nonaqueous electrolytes are used and the cathode half-reaction is appropriately selected, it is possible to increase the standard potential of the cell to 3–3.5 V, and high redox capacity of lithium metal may increase the stored energy density severalfold in comparison with VRFBs.

Wei *et al.*[92] filled the anode compartment with a lithium–carbon hybrid material based on carbon felt, which served as an intercalation anode. A solution of $LiPF_6$ in a mixture of ethylene carbonate, propylene carbonate and ethyl methyl carbonate was used as the supporting electrolyte. During RFB charging, the Li^+ ions were intercalated into the anode material, while the discharge was accompanied by the reverse deintercalation process. In the cathode compartment, TEMPO dissolved in the same electrolyte was used (the TEMPO concentration varied from 0.1 to 2.0 M). A porous membrane based on polyethylene was meant to transport Li^+ ions for maintaining the balance; see Fig. 3 and Eqns (23)–(25).

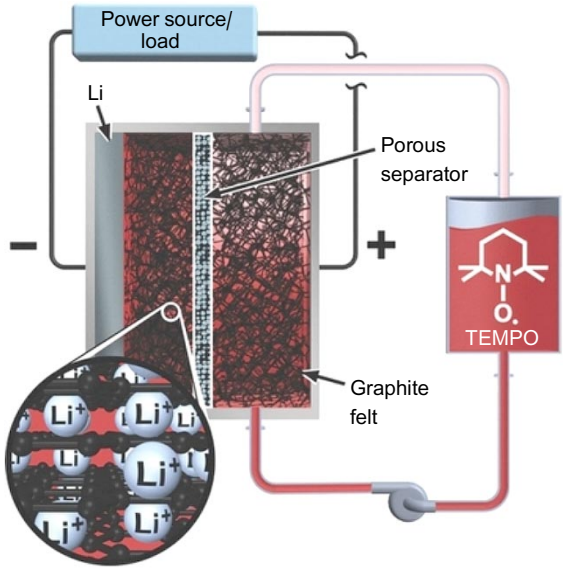


Figure 3. Basic diagram of Li/TEMPO hybrid RFB. Reproduced from Ref. 92 with the permission of Wiley-VCH.

The reaction on the positive electrode

$$TEMPO^{\bullet} \leftrightarrows TEMPO^{+} + e^{-};\ E_0 = 0.80\ V \quad (23)$$

The reaction on the negative electrode

$$Li^{+} + e^{-} \leftrightarrows Li;\ E_0 = -3.04\ V \quad (24)$$

The overall reaction

$$TEMPO^{\bullet} + Li^{+} \leftrightarrows TEMPO^{+} + Li;\ E_{cell} = -3.84\ V \quad (25)$$

The standard potential of this cell was 3.8 V, and for the maximum possible TEMPO solubility, this corresponds to a theoretical energy density of 188 W h L^{-1}. In practice, an energy density of 126 W h L^{-1} was attained using a current density of 1 mA cm^{-2}. The coulombic, voltaic and energy efficiencies were 84, 82 and 69%, respectively. As the catholyte concentration decreased to 0.8 M, the charge–discharge current densities increased to 10 mA cm^{-2}; however, this value is still several orders of magnitude lower than analogous values accessible for VRFBs. This drawback of lithium redox flow batteries was attributed to hindered transport of Li^+ ions through the membrane.

Meanwhile, the specific energy density can be increased by further selection of the catholyte. Takechi *et al.*[93] employed a mixture of 4-MeO-TEMPO with 1 M plasticizing salt, lithium bis(trifluoromethanesulfonyl)imide LiTFSI. This salt possesses a self-melting effect and, therefore, there is no need to add a large volume of the solvent. A mixture with 1 : 1 volume ratio of the components containing 17 mass % of water was used. The anode was made of lithium metal and the anode compartment was filled by 1 M LiTFSI as the supporting electrolyte; and a lithium permeable ceramic membrane was used as the separator. The theoretical stored energy density for this RFB was as high as 200 W h L^{-1}; however, the charge–discharge cur-

rent densities attainable during operation still did not exceed 1 mA cm^{-2}.

3.2.4. Hydrogen halogen RFB

In addition to liquid and solid compounds, gases can also act as electroactive RFB components. These systems are called hybrid, because they combine a gas half-cell of a fuel cell and a liquid RFB half-cell. The best developed batteries of this type are hydrogen halogen RFBs. During the discharge, gaseous hydrogen is oxidized on the negative electrode (often, the electrode surface is modified by noble metal electrocatalysts), while on the positive electrode, molecular X_2, where X is a halogen atom, is reduced from an aqueous solution of HX. A basic diagram of the system is shown in Fig. 4; the reactions are described by Eqns (26)–(28).

The reaction on the negative electrode

$$2H^+ + 2e^- \leftrightarrows H_2;\ E_0 = 0.00\ \text{V (in acid medium)} \quad (26)$$

The reaction on the positive electrode

$$2X^- \leftrightarrows X_2 + 2e^-;\ E_0 = 0.54\ (I_2);\ 1.09\ (Br_2);\ 1.36\ (Cl_2)\ \text{V} \quad (27)$$

Thr overall reaction

$$2HX \leftrightarrows X_2 + H_2 \quad (28)$$

The key benefits of hydrogen halogen RFBs include high rate and reversibility of the redox reactions of the X_2/X^- couple and the use of inexpensive reactants. The Cl_2/Cl^- and Br_2/Br^- standard potentials are 1.36 and 1.09 V, respectively, while that for the I_2/I^- couple is 0.54 V. Therefore, Cl_2 and Br_2 are considered to be the most promising halogens for hydrogen halogen RFBs. The F_2/F^- redox couple possesses an even greater standard potential (E_0 = 3.05 V *versus* SHE); however, hydrogen fluorine RFB is hardly practicable, due to the difficulties associated with handling of gaseous fluorine.

The interest of researchers is focused on the H_2/Br_2 flow battery. This battery showed discharge power densities at 1.4–1.5 W cm^{-2} level,[94,95] while in 2015, the Enstorage Inc. company (Israel) constructed and launched an experimental industrial prototype of hydrogen bromine RFB with the maximum power of 150 kW and energy storage capacity of 900 kW h.[96–98]

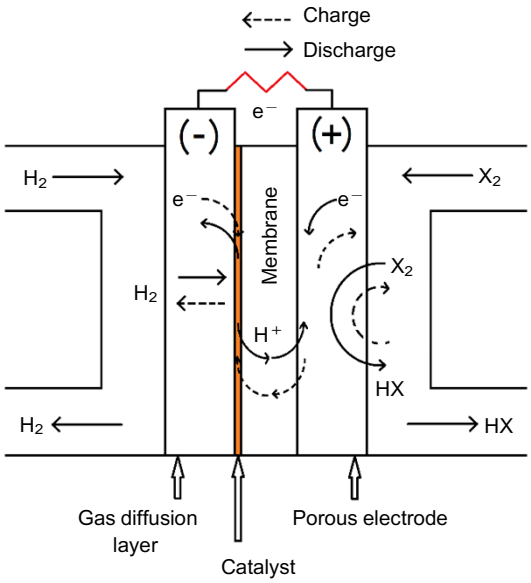


Figure 4. Basic diagram of hydrogen halogen RFB.

However, hydrogen bromine RFBs also have a number of drawbacks:[99]

— high cost of anodes with a catalytic layer;

— high reactivity and toxicity of halogen-based catholytes, which reduces the durability and safety of the system;

— intense crossover of halogen compounds, resulting in decreasing efficiency and degradation of expensive catalysts for hydrogen oxidation.

Considering the listed drawbacks, an important role belongs to the limited stored energy density of hydrogen bromine RFBs, which is theoretically estimated[100] as not exceeding 354 W h L^{-1} (this is explained by the limited solubility of bromine in water under standard conditions). This value exceeds analogous characteristics of VRFBs by a large factor, but it is still markedly inferior to the theoretical energy density of lithium-ion batteries.

Thus, hybrid RFBs of type I combine the potential of classic RFBs with benefits of other types of CPS. The use of intercalation electrodes considerably increases the maximum energy density of lithium redox flow batteries, while hydrogen halogen RFBs, which combine the principles of redox batteries and fuel cells, have higher power density than other types mentioned above. Meanwhile, hybrid RFBs lose some advantages of classic flow batteries. For example, in zinc bromine RFBs and lithium flow batteries, the power and capacity characteristics are no longer independently scalable.

Nevertheless, some hybrid RFBs are already being tested or even used under real conditions (see zinc bromine RFB and hydrogen halogen RFBs). In addition, in recent years, active laboratory studies have been devoted to energy storage systems that are based on the common RFB concept, but it is so highly modified that these storage systems can hardly be assigned to usual hybrid RFBs. These studies are summarized below in the Section called 'Hybrid RFBs, type II.'

3.3. Hybrid RFBs, type II

3.3.1. RFBs using redox mediators

Hydrogen bromate RFB. As shown in 2015 by Tolmachev,[101] the replacement of halogen solutions by solutions of halogen oxoacids as the catholyte may bring about a severalfold increase in the stored energy density compared to the energy density observed for hydrogen halogen RFBs. Aqueous solutions of bromates provide a high theoretical energy density due to combination of high solubility (*e.g.*, the solubility of $LiBrO_3$ is 4.5 to 5.8 mol per kg of the solution for temperatures from −40 to 100 °C, respectively) and six-electron conversion of the bromate to bromide anion. Also, high solubility is inherent in the products of reduction of this catholyte, such as LiBr.

In addition, halogen oxoacids have high chemical stability and low toxicity compared to molecular halogens and are produced using cheap and readily available starting materials, and their cathode reactions do not require expensive catalysts. Theoretically, these factors altogether provide very low unit cost of the produced electricity.

However, neither bromate anions nor other halogen oxoacid anions were considered in electrochemical energy production for a long time, because of their low electrochemical activity. Their electroreduction proceeds at a high rate only at high overpotential even on noble metal electro-

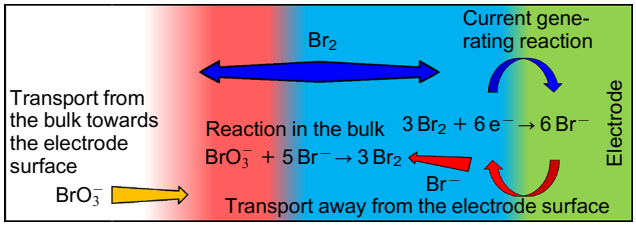


Figure 5. Schematic view of homogeneous and heterogeneous reactions taking place in the positive electrode half-cell of a hybrid hydrogen bromate RFB.

des, which made the use of cathode reactions for electrical energy storage almost meaningless.

However, as shown,[101, 102] high rates of reduction of bromate anions still can be attained when the electroreduction of molecular bromine [see equation (20)] taking place on the electrodes without additional catalysts is combined with homogeneous conproportionation taking place in solution (see Fig. 5):

$$BrO_3^- + 5\,Br^- + 6\,H^+ \rightarrow 3\,Br_2 + 3\,H_2O \quad (29)$$

As the reaction cycle (20) and (29) is repeated, the bromate anion is gradually converted to bromide, which corresponds to the overall equation

$$BrO_3^- + 6\,e^- + 6\,H^+ \rightarrow Br^- + 3\,H_2O \quad (30)$$

Since the reduction of bromate anions is a six-electron reaction and the solubility of $LiBrO_3$ amounts to 4.9 mol kg^{-1} and 5.5 mol kg^{-1} for 25 and 60 °C, respectively,[103, 104] the specific capacity of a saturated solution of lithium bromate is 790 A h kg^{-1} at 25 °C and 880 A h kg^{-1} at 60 °C.

For reaction (29), E_0 = 1.41 V *versus* SHE.[105] In combination with the anodic hydrogen oxidation reaction (26) and assuming that the mass fraction of hydrogen in the hydrogen storage tank is 5.7 mass %,[106] one gets that the specific capacities of a hydrogen bromate RFB are 520 and 560 A h kg^{-1} at 25 and 60 °C, respectively, and the energy densities are 750 and 810 W h kg^{-1} at 25 and 60 °C, respectively. These values are markedly superior to the analogous values for many types of RFBs mentioned above.

Hydrogen bromate RFBs also suffer from some shortcomings. First, mention should be made of the complexity of this system and a low level of knowledge of the kinetics of cathode reactions and the reactant transport in the cathode region, which are unusual for RFBs, since a heterogeneous electrochemical reaction and a homogeneous chemical reaction take place simultaneously. Second, an efficient hydrogen bromate RFB requires high concentrations of halogen-containing reactants and simultaneously low pH value; this gives rise to severe restrictions to practical implementation of this concept. In the design of MEA for a hydrogen bromate RFB, it is necessary to take into account high corrosivity of bromine vapour. Furthermore, the selection of the battery operating mode requires sophisticated optimization taking account of the nonmonotonic pattern of reactions (20) and (29). In addition, the composition of bromate catholyte should be adjusted in such a way as not to exceed the solubilities of redox couple components accumulated during RFB operation.

Nevertheless, the prospects for using aqueous solutions of bromate anions as catholytes were practically confirmed by a study of Vorotyntsev's research group,[107] in which the authors fabricated a laboratory prototype of a hydrogen bromate cell with an active surface area of 50 cm^2 and a power density of 0.9 W cm^{-2} (at a current density of 1.5 A cm^{-2}). These results were supported by independent testing at the Laboratory of Electrocatalysis of the Frumkin Institute of Physical Chemistry and Electrochemistry, Russian Academy of Sciences and laboratory of the InEnergy company.

Other flow systems with redox mediators. In a hydrogen bromate RFB, Br_2 acts as a redox mediator, while the BrO_3^- anion is a non-electroactive compound that reacts with components of the cathode redox couple and thus increases the stored energy density severalfold. A similar approach is often used for other systems, for example, for various lithium flow batteries.

In a study of Zhu *et al.*,[108] tetramethylphenylenediamine (TMPD) was utilized as a redox mediator in the cathodic half-cell reaction, and $LiFePO_4$ was added to the cathode tank as solid granules. Only the cathodic compartment had a circuit for electrolyte circulation. A TMPD solution in diethylene glycol dimethyl ether was circulated between the cathodic copmpartment and the tank; 0.5 – 1 M LiTFSI was used as the supporting electrolyte. In the anodic compartment, lithium foil was used as the negative electrode and no electrolyte circulation was present. A Nafion/polyvinylidene fluoride (1 : 1) composite membrane was used as a separator. The reactions taking place in the cell are described by Eqns (31) – (36).

Charging on the positive electrode

$$TMPD^{\bullet+} \rightarrow TMPD^{\bullet 2+} + e^- \quad (31)$$

Charging in the cathode tank

$$TMPD^{\bullet 2+} + LiFePO_4 \leftrightarrows TMPD^{\bullet+} + Li^+ + FePO_4 \quad (32)$$

Discharge on the positive electrode

$$TMPD^{\bullet+} + e^- \rightarrow TMPD \quad (33)$$

Discharge in the cathode tank

$$TMPD^{\bullet+} + Li^+ + FePO_4 \rightarrow TMPD^{\bullet+} + LiFePO_4 \quad (34)$$

The reaction on the negative electrode

$$Li^+ + e^- \rightarrow Li;\ E_0 = -3.04\ V \quad (35)$$

The overall reaction

$$LiFePO_4 \leftrightarrows Li + FePO_4 \quad (36)$$

With the assumed maximum concentration of TMPD (0.5 M) and maximum effective concentration of Li^+ ions in the $LiFePO_4$ granules (22.8 M at 50% porosity of $LiFePO_4$), the theoretical energy density in the system can reach 1023 W h L^{-1}; in our opinion, this is the record-high value among all RFBs. In practice, the TMPD concentration was 25 mM, which corresponds to a specific discharge capacity of 160 mA h g^{-1}. The power density was 61 mW cm^{-2} (testing was carried out in an undivided cell). It should be noted that this system demonstrated moderate characteristics in charge – discharge cycling. When the current density was 0.125 mA cm^{-2}, the coulombic efficiency was 76%, which is attributable to degradation of the redox mediator at high voltage: as the upper voltage limit decreased, the coulombic efficiency increased to ~100%; however, simultaneously, the $LiFePO_4$ utilization ratio nearly halved (decreased from 73 to 40%).

The selection of optimal redox mediators is a key aspect of these studies: the mediators should be stable during charge–discharge cycling and undergo the target reactions without considerable overpotential. When TMPD is replaced by I^-, with other key constituents (anode material, supporting electrolyte, general principle of the unit) being the same (Fig. 6), the system stability markedly increases. For 40 charge–discharge cycles with a current density of 0.075 mA cm^{-2}, the coulombic efficiency was ~99% and the overall capacity retention rate was ~90%.[109] However, with the theoretical energy density in this system (2 M solubility of LiI and 50% porosity of $LiFePO_4$) being 670 W h L^{-1}, in practice, the discharge capacity of only 0.8 mA h was demonstrated using 10 mM LiI.

Non-electroactive compounds that increase the system capacity may present not only in the cathode part, but also in the anode part or in both parts. Jia *et al.*[110] used the ferrocene redox couple in the cathode half-cell and the cobaltocene redox couple in the anode half-cell. A 1 M LiTFSI solution in tetraethylene glycol dimethyl ether served as the supporting electrolyte; TiO_2 and $LiFePO_4$ were used as solid components of the anode and cathode tanks, respectively; carbon felt was used as the cathode, nickel foam acted as the anode, and the Nafion/PVDF composite functioned as the separator. The maximum theoretical energy density of this RFB was 500 W h L^{-1}, the average discharge voltage was 1.25 V and the peak charge density was 250 A h L^{-1}.

It is noteworthy that the authors of the cited study refused to use lithium metal anodes, which are employed in many other lithium RFBs; however, the half-reactions were still balanced by the transport of Li^+ cations through the membrane. This dictates a few specific requirements to the separator material: it should be mechanically and chemically stable, prevent intense crossover of components of mediator redox couples and simultaneously provide considerable Li^+ ion mobility. In the general case, characteristics of redox mediator RFBs can be limited by three key processes: kinetics of heterogeneous reactions of redox mediators on the electrode surface; kinetics of homogeneous chemical reactions of redox mediator components with non-electroactive compounds in the bulk of the tanks; and lithium cation transport across the membrane. In all of the studies mentioned above, the last-mentioned process was the limiting one and the highest charge–discharge currents did not exceed 0.1–0.15 mA cm^{-2}, which is critically low for the practical use of RFBs.

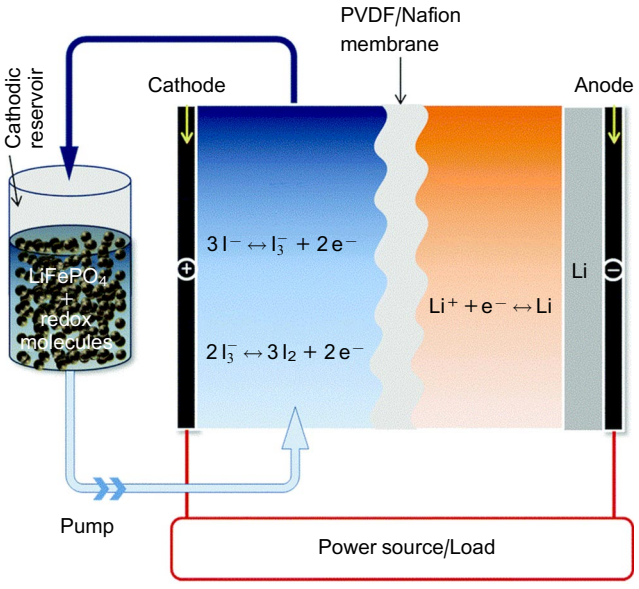


Figure 6. General scheme of lithium iodide RFB with a redox mediator. Reproduced from Ref. 109 with the permission of the Royal Society of Chemistry.

Meanwhile, the redox mediator approach can also do without lithium chemistry. For example, Zhou *et al.*[111] used polyimides in the anode tank and AQDS as the redox mediator (the theoretical energy density was 39 W h L^{-1}), and Preger *et al.*[112] also employed AQDS as the redox mediator for the anodic H_2 oxidation reaction. Cheng *et al.*[113] combined the classic VRFB principle with the use of granular Prussian blue analogue in the cathode tank. This increased the theoretical specific capacity of VRFB to 135 A h L^{-1}, whereas the value demonstrated in practice was 44.6 A h L^{-1}, which exceeds only slightly the values inherent in conventional VRFBs. The use of a redox mediator made it possible to attain these characteristics against a decrease in the concentration of vanadium-containing components in the system (50 mL of 0.6 M V^{+2}/V^{+3} was used as the anolyte and 20 mL of 0.6 M VO^{2+}/VO_2^+ was used as the catholyte). As a result, the temperature range of the system was extended up to + 70 °C. In addition, the charge–discharge current density was 30 mA cm^{-2}, which exceeds the maximum current density typical of lithium redox mediator systems by a large factor.

Thus, the use of redox mediators in RFBs offers a lot of opportunities for increasing the stored energy density, but currently it is associated with a number of challenges: it is necessary to thoroughly select redox mediators taking account of a variety of requirements and membrane materials.

3.3.2. Suspension RFBs

Electroactive components can be used in RFBs not only as liquids, gases or solids, but also as suspensions (slurries). These RFBs can be classified into two groups: those using polymer suspensions and those using semisolid electrodes.

RFBs with polymer suspensions. Redox active polymers used as electroactive RFB components have a number of advantages. First, a large size of macromolecules eliminates the need for expensive membranes. Second, the role of crossover is minimized, which substantially increases the RFB cycle life. In addition, the use of electrically conducting (or conjugated) polymers decreases the cell resistance, which is also beneficial for RFB characteristics. However, there is the problem of low solubility of these compounds in aqueous media, which substantially decreases the stored energy density. Meanwhile, the use of nonaqueous electrolytes leads to lower mobility of the balancing counterions across the separators, and this reduces the power characteristics and restricts the range of applicable charge–discharge current densities.

One solution to this problem is the use of stable polymer suspensions instead of true solutions. For example, Zhao *et al.*[114] reported an RFB using a suspension of polyaniline (PANI) microparticles (150 g L^{-1}) in aqueous 2 M $ZnCl_2$ and 2 M NH_4Cl solutions as the catholyte. The anode was represented by zinc metal on which zinc electrodeposition/dissolution took place. A readily available microporous polypropylene-based membrane served as the separator.

The reactions that take place in the system are described by Eqns (37)–(39).

The reaction on the positive electrode

$$2\,\mathrm{PANI} \leftrightarrows 2\,\mathrm{PANI}^{+} + 2\,\mathrm{e}^{-};\ E_0 = 0.39\ \mathrm{V\ (SHE)} \qquad (37)$$

The reaction on the negative electrode

$$\mathrm{Zn}^{2+} + 2\mathrm{e}^{-} \leftrightarrows \mathrm{Zn};\ E_0 = -0.76\ \mathrm{V\ (SHE)} \qquad (38)$$

The overall reaction

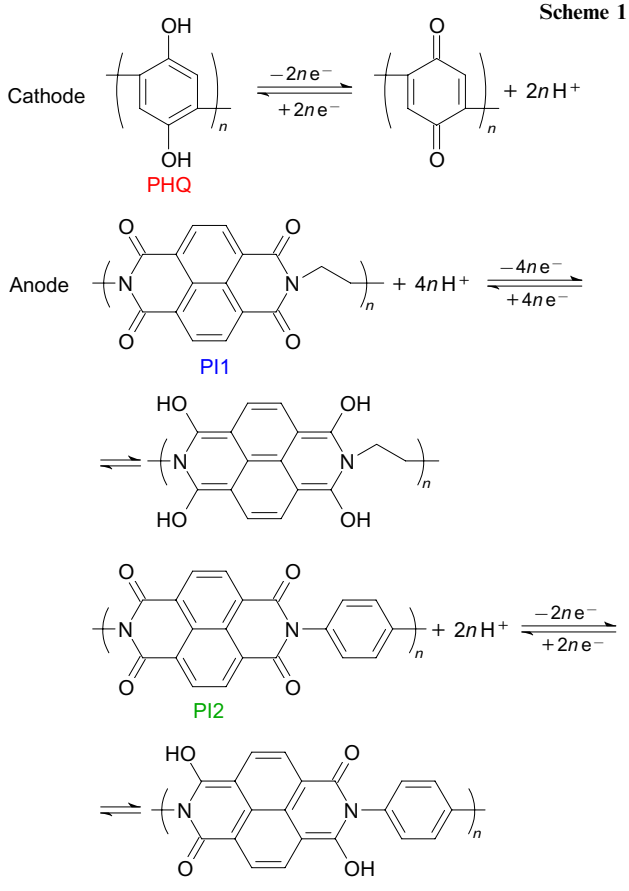
$$\mathrm{Zn}^{2+} + 2\,\mathrm{PANI} \leftrightarrows 2\,\mathrm{PANI}^{+} + \mathrm{Zn};\ E_{\mathrm{cell}} = 1.15\ \mathrm{V} \qquad (39)$$

The device demonstrated a stored energy density of 9.5 W h L^{-1}, with the theoretical value being 66.5 W h L^{-1}. The average discharge voltage was 1.1 V. For 32 charge–discharge cycles with a current density from 10 to 30 mA cm^{-2}, the average coulombic efficiency was 97%, while the capacity retention rate was 99.93% per cycle.

Polymer suspensions can be simultaneously used in both RFB half-reactions. For example, a stable polyhydroquinone PHQ suspension (in 1 M concentration in terms of monomer units) in 2 M H_2SO_4 was used as the catholyte and PI1 and PI2 polyimide derivatives acted as the anolyte.[115] The use of two polymer suspensions gave rise to an RFB with a separator based on a cheap dialysis membrane, through which the balancing counterions diffused. The structures of the used chemicals and the reaction equations are depicted in Scheme 1.

During charge–discharge cycling at a current density of 20 mA cm^{-2}, the device demonstrated a specific capacity of 3.95 A h L^{-1} and the energy density of 1.98 W h L^{-1}. The coulombic, voltaic and energy efficiencies were 99.1, 58.6 and 58.1%, respectively. This low voltaic efficiency and, as a consequence, low energy efficiency are attributable, first of all, to limitations of electron transfer on the surface and inside polymer aggregates. Also, this RFB showed good stability characteristics: for 5000 charge–discharge cycles, the capacity retention rate was 99.995% per cycle.

Scheme 1



It should be specially mentioned that the composition of polymer suspensions to be used as RFB electrolytes should be carefully selected: first, they must demonstrate a reasonable rate of redox transitions, and, second, they must remain stable for long periods of time. For example, pure aqueous suspensions of PHQ and PI1/PI2 precipitate soon after the preparation and are stabilized only by addition of H_2SO_4. The use of polymer suspensions is also faced with other complications. The major one is high viscosity of polymer electrolytes, resulting in high power consumption for pumping and frequent clogging of flow channels. In addition, the standard potential of redox couples based on electroactive polymers changes depending on the state of charge, which leads to very high curvature of the E_{cell} (SOC) dependence at the edges of SOC range and, hence, strongly restricts the possibility of using the whole available capacity in the storage systems based on polymer suspensions.

RFBs with semisolid electrodes. The key idea of the semisolid electrodes is the fabrication of suspensions combining functions of redox-active electrolytes and electrodes. First, this may increase the stored energy density of the system by a large factor without the use of redox mediators and, second, this may decrease the capital cost for the manufacture of RFBs: instead of expensive polymer membranes, it is possible to use cheaper separators, and there is no need for solid electrodes, because all redox reactions proceed on the surface of electroconductive aggregates dispersed in the bulk.

The general concept was proposed in 2011 by Professor Y.-M.Chiang's research group from the Massachusetts Institute of Technology (Cambridge, USA).[116] The authors studied various electrolyte compositions; the optimal characteristics were found for the following pair: a suspension of electroactive $LiCoO_2$ (20 vol.%, effective concentration of 10.2 M) in nonaqueous supporting electrolyte (1 M $LiPF_6$ in a mixture of alkyl carbonates) with electrically conductive additive based on Ketjenblack (KB) carbon nanoparticles (1.51 vol.%) as the catholyte and a $Li_4Ti_5O_{12}$ suspension (10 vol.%, effective concentration of 2.3 M) in the same supporting electrolyte + KB additive (2 vol.%) as the anolyte. The Celgard 2500 microporous polymer separator with an average pore size <0.1 μm was used.

The maximum effective concentrations of Li^+ in $LiCoO_2$ and $Li_4Ti_5O_{12}$ are 51.2 M and 22.6 M, respectively. This is tens of times higher than the corresponding value for VRFB (the characteristic concentrations of electroactive components are not higher than 1.7–2 M). Considering the average discharge voltage of 2.35 V and assuming that the concentrations of electroactive components are 40 vol.%, the theoretical energy density in this system amounts to 397 W h L^{-1}. However, the practical implementation of these opportunities is associated with difficulties. For example, the coulombic efficiency of this system is 80% even in the first cycle and 73% in the second cycle, which is due to the considerable contribution of side chemical reactions (most of all, oxidation with atmospheric oxygen).

The first fundamental difficulty in the fabrication of semisolid electrodes is the selection of the optimal composition of the suspension, on which numerous requirements are imposed. On the one hand, a stable percolation struc-

ture of conducting particles should exist in such systems; on the other hand, it is necessary to increase as much as possible the number of accessible electroactive particles, and the system should possess appropriate rheological properties, show a high rate of redox transitions, have high electronic and ionic conductivity and remain stable during charge–discharge cycling. These requirements largely contradict one another and need to be thoroughly investigated.

The choice of electrolyte circulation regime is also a challenge. Semisolid electrodes are non-Newtonian liquids, for which the optimal electrolyte flow rates are moderate: a few mL per minute *versus* tens of mL per minute used in other systems. Even discrete (portionwise) delivery may be required. Li *et al.*[117] used a $LiFePO_4$ suspension (10 vol.%) in 1 M aqueous solution of $LiNO_3$ (pH = 11–12) containing 1.5 vol.% KB as the catholyte and $LiTi_2(PO_4)_3$ (18 vol.%) + KB (2 vol.%) + the same supporting electrolyte as the anolyte. With the optimized discrete electrolyte pumping regime (the effective flow rate was 30 μL s^{-1}), 10 charge–discharge cycles resulted in coulombic and energy efficiency of 90 and 75%, respectively, which exceeds the values mentioned above. It is also noteworthy that in the cited study,[117] suspensions were prepared in an aqueous electrolyte, unlike those in the study of Duduta *et al.*[116]

A key factor is that semisolid electrodes should not necessarily be used for both half-reactions. Yang *et al.*[118] employed sodium melt as the anode and a suspension of sulfur particles in the presence of 1 M NaI in a nonaqueous solvent + 2 vol.% KB as the semisolid electrode/catholyte (for block diagram, Fig. 7). The specific capacity of this system reached 864 mA h g^{-1} in the first operation cycles.

Finally, Chen *et al.*[119] used lithium metal as the anode and a suspension of sulfur particles (20 vol.%, effective concentration of 12.9 M) + KB (26 vol.%) in the presence of a complex supporting electrolyte (0.2 M $LiClO_4$ + 0.1 M $LiNO_3$ in a 1 : 1 1,3-dioxolane and 1,2-dimethoxyethane mixture) as the catholyte/semisolid cathode. A polymer membrane was used as the separator.

Currently, this is one of the most successful studies devoted to semisolid electrodes from the standpoint of RFB characteristics. The theoretical specific capacity of the cell was 670 A h L^{-1}, whereas in the static cell regime (the absence of electrolyte circulation), this value was 294 A h L^{-1}. During 100 charge–discharge cycles carried out at a current density of 6 mA cm^{-2}, the coulombic efficiency varied from 90.3 to 94.5%, the energy efficiency was 82 to 83.7% and the overall capacity retention was 85%. These characteristics were due to the optimized structure of the catholyte, which was prepared by high-temperature treatment rather than by mere physical mixing of components, as in other works. As a result of this treatment, sulfur particles were incorporated into the percolation carbon structure, which substantially improved the electrical contact and decreased the viscosity of the suspension catholyte.

Thus, the fabrication of efficient semisolid electrodes is able to considerably reduce the capital cost of RFB design, while the specific capacity of RFBs increases by a large factor. However, this requires highly labour-intensive selection of compositions for the suspensions and optimization of circulation conditions in the cell, and currently the potential of this approach has not yet been fully implemented.

3.3.3. RFBs using additional flow circuits and/or cells

Traditionally, an RFB has two tanks (one for the catholyte and one for the anolyte), two electrolyte circuits and one membrane electrode assembly. In RFBs with metal (zinc, lithium, molten sodium) anode, there is only one circuit and one electrolyte tank. However, opposite design modifications such as additional cells, flow circuits or electrolyte tanks included in the RFB are also possible.

Jiang *et al.*[120] proposed an VRFB with two MEAs, one for electrolyte charging and one for discharge (Fig. 8). This design allowed separate optimization of the structure of each cell, which resulted in a unique enhancement of VRFB characteristics.

A 50 μm-thick Nafion 212 membrane, possessing low permeability for redox couple components, was used in the charging assembly. The following requirements were imposed on the charging assembly electrodes: a large active surface area and, simultaneously, a large number of oxygen-containing functional groups that facilitate the V^{3+} to V^{2+} reduction. According to these requirements, highly active heat-treated felt served as the positive electrode and a similar Pb-modified material acted as the negative electrode.

In the discharge assembly, a 25 μm-thick Nafion 211 membrane was used. If the system had only one MEA, the

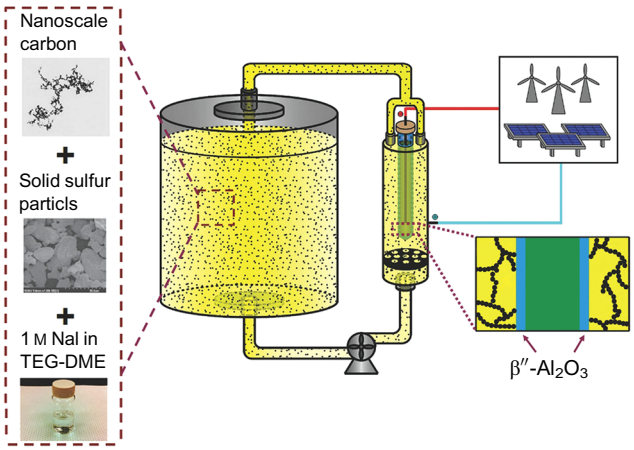


Figure 7. Basic diagram of sodium iodide suspension RFB. Reproduced from Ref. 118 with the permission of Wiley-VCH.

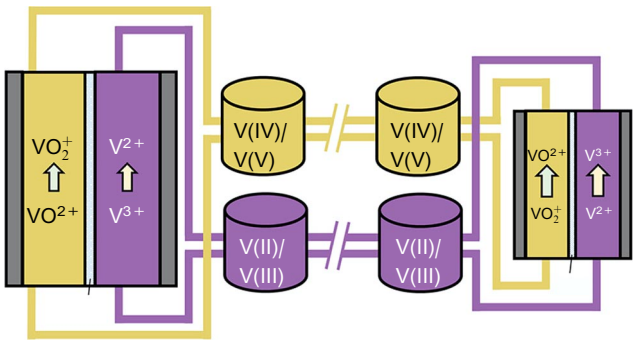


Figure 8. Basic diagram of a vanadium energy storage device with separated charge and discharge assemblies. Reproduced from Ref. 120 with the permission of Elsevier B.V.

application of such thin membrane would result in intense crossover of vanadium compounds and, as a consequence, high system imbalance on long-term operation. However, discharge can be performed much faster than charging (by using high current density and high rates of electrolyte delivery) and, hence, in the separate discharge assembly, the small thickness of the membrane does not cause adverse effects, but, conversely, it is a beneficial factor, minimizing the cell resistance and thus increasing the power. Heat-treated carbon felt served as the positive electrode of the discharge assembly, while an identical material additionally modified by bismuth was used as the negative electrode.

The anolyte was represented by 1.07 M V^{3+} in 3 M H_2SO_4, while the catholyte was 1.07 M VO^{2+} in 3 M H_2SO_4. The electrolyte flow rate was 50 mL min^{-1} in the charging MEA and 80 mL min^{-1} in the discharge assembly. The power density of the system was 2.75 W cm^{-2} at 25 °C (for current density of 3.2 A cm^{-2}) and 3.4 W cm^{-2} at 55°C (corresponds to the current density of 4.2 A cm^{-2}). As the current density in the discharge assembly was varied from 400 to 1200 mA cm^{-2}, the capacity utilization rate decreased from 95 to 80%. During 100 charge–discharge cycles (with a current density of 60 mA cm^{-2} in the charging MEA and 600 mA cm^{-2} in the discharge MEA), the coulombic efficiency varied from 97 to 99% and the charge density was in the range from 11 to 13 A h L^{-1}.

Thus, the separation of the discharge and charging RFB units significantly enhanced some of the key characteristics of classic VRFBs (maximum discharge power, the range of allowable discharge current densities and, as a consequence, the characteristic discharge time). According to the authors, this led to a significant decrease in the capital cost for the manufacture of the energy storage device per kW h.

By using several additional flow circuits, it is also possible to increase the stored energy density of RFBs by means of additional products such as gaseous hydrogen and oxygen.[121] A typical example of such systems was reported by Amstutz *et al.*,[122] who used additional external flow circuits for catalytic electrolysis of water, in parallel with the central RFB circuits (Fig. 9).

This RFB can function as a conventional RFB; however, when liquid electrolytes are fully charged, a discharge process starts in the external circuits of catalyzed water splitting to generate H_2. The fully charged catholyte and anolyte are pumped to the corresponding circuits and participate in oxygen and hydrogen evolution reactions as the electron acceptor and donor, respectively. This engineering solution provides storage of more energy. Some of the energy is stored as the chemical energy of liquid electrolytes, while the surplus energy is stored as gaseous hydrogen, which can be used in other current sources.

Unlike other electrolytic cells for the generation of hydrogen, in this case, the catalytic water splitting reaction proceeds in a separate part of the energy storage device and does not depend on electrochemical processes taking place in the central battery MEA. As a result, O_2 and H_2 recombination and electrode degradation are avoided and the use of catalysts based on expensive noble metals is minimized.

It is also noteworthy that with this approach, charged electrolytes can be used not only for indirect electrolysis of water, as in the above example or in other studies,[122] but also for other reactions, *e.g.*, for the conversion of SO_2 and H_2S to S and H_2SO_4.[123]

The main difficulties faced by implementing this system are as follows:

— complexity of selecting the balancing redox reaction for the second external circuit to implement the indirect water electrolysis to H_2;

— arranging the catalytic reactors. The catalysts should meet numerous requirements: high activity, stability, relatively low cost, *etc.*;

— the complexity of the system design. It is necessary to connect quite a few parts: RFB and the tanks and electrolytes pipings; two external flow circuits for charged electrolytes and the catalytic reactors and/or flow electrochemical cells, a hydrogen storage tank, *etc.*

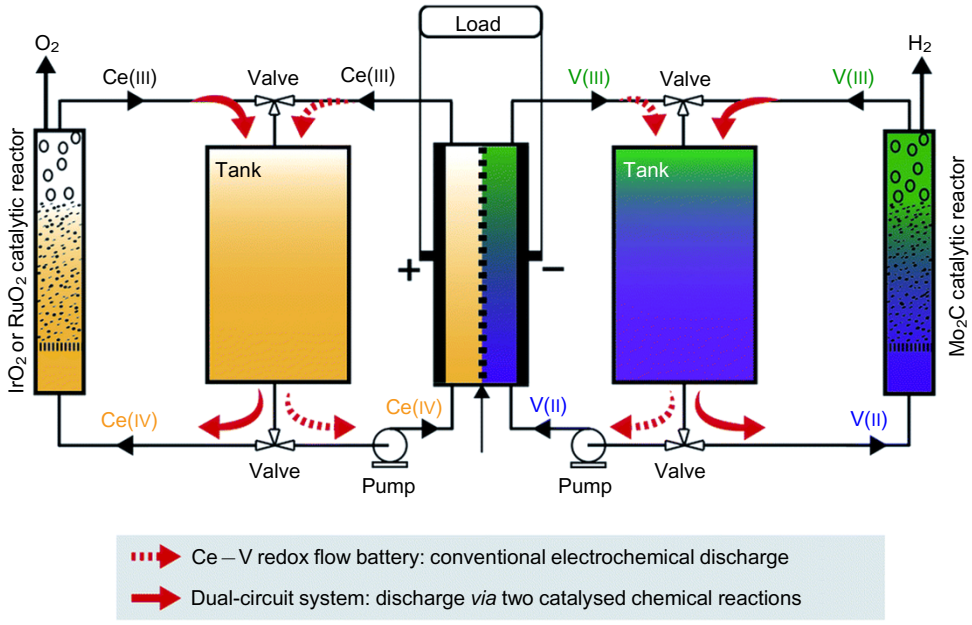


Figure 9. Example of RFB with additional flow circuits. Reproduced from Ref. 122 with the permission of Royal Society of Chemistry.

Currently, there are no prototypes of such systems ready for industrial application. Piwek *et al.*[124] presented a concept of a fully balanced system based on such RFBs; however, to date it was tested only on a laboratory scale.

3.3.4. RFBs using auxiliary processes

Acid–base RFBs. The possibility of fabricating an electrical energy storage system with a bipolar membrane using the energy of neutralization reaction between an acid and an alkali was first proposed in 1971.[125] The first experimental study of CPS based on this concept was carried out in 1979.[126] Later, data on a single cell with a bipolar membrane,[127] a mathematical model[128] and a study of the effect of membrane characteristics on the parameters of flow battery[129] were reported. The interest in this type of energy storage devices was revived only in 2016,[130] in relation to the search for more environmentally safe and readily available electrolytes for RFBs.

In these RFBs, electricity is generated through a neutralization reaction between an acid and an alkali. The electrolytes are solutions of an acid, an alkali and a salt, which are circulated in their compartments separated by cation- and anion-exchange and bipolar membranes (Fig. 10). On both ends of the cell, electrodes are located in the corresponding compartments and a solution of the electroactive component is circulated between the electrodes, thus closing the circuit. During the discharge of the acid–base battery, concentrated solutions of acid and alkali are neutralized, and simultaneously the concentration of the salt solution increases. The electroactive component solution is circulated in the closed circuit, being oxidized on one electrode and reduced on the other electrode. As an example, below are given reactions (41)–(43) corresponding to the discharge of an acid–base RFB in which water electrolysis is used as a redox reaction.[131]

The reaction on the negative electrode

$$1/2\,H_2O \leftrightarrows H^+ + 1/4\,O_2 + e^- \quad (40)$$

The reaction on the positive electrode

$$e^- + H_2O \leftrightarrows OH^- + 1/2\,H_2 \quad (41)$$

The overall reaction

$$H_3O^+ + OH^- \leftrightarrows 2\,H_2O \quad (42)$$

As redox couples, pH-sensitive systems, *e.g.*, $H^+/H_2O/OH^-$ (Refs 130–132), H_2/H^+ (Ref. 125), Fe^{2+}/Fe^{3+} (Ref. 134) and other, can be used. Xia *et al.*[133] presented a single cell of an acid–base battery with 0.25–1 M HCl and NaOH, 0.5 M NaCl and 0.25 M Na_2SO_4 solutions, FKB, FAB and FBM membranes (Fumatech BWT GmbH) and platinum electrodes. Water electrolysis was used as the redox reaction. Kim *et al.*[134] studied a system with 0.1–0.7 M NaOH, 0.01 M NaCl and 0.1 M Fe^{2+}/Fe^{3+} solutions in 0.1 M Na_2SO_4, CMS/CMX, AM-1 and BP-1 membranes (Tokuyama Inc.) and carbon cloth and platinized titanium electrodes. A power density from 0.6 (at 1.7 mA cm^{-2} for 0.1 M) to 1.05 mW cm^{-2} (at 3 mA cm^{-2} for 0.6 M) was demonstrated. When 13 charge–discharge cycles were conducted with a current density of 0.29 mA cm^{-2} and potential ranging from 0.4 to 1.25 V, the efficiency values remained stable during eight cycles (the coulombic efficiency was 93–100% and the voltaic efficiency and energy efficiency ranged from 72 to 80%).

It is noteworthy that, apart from a three-membrane cell, an acid–base battery may be designed to have one membrane and two electrolytes. Saez *et al.*[130] reported an acid–

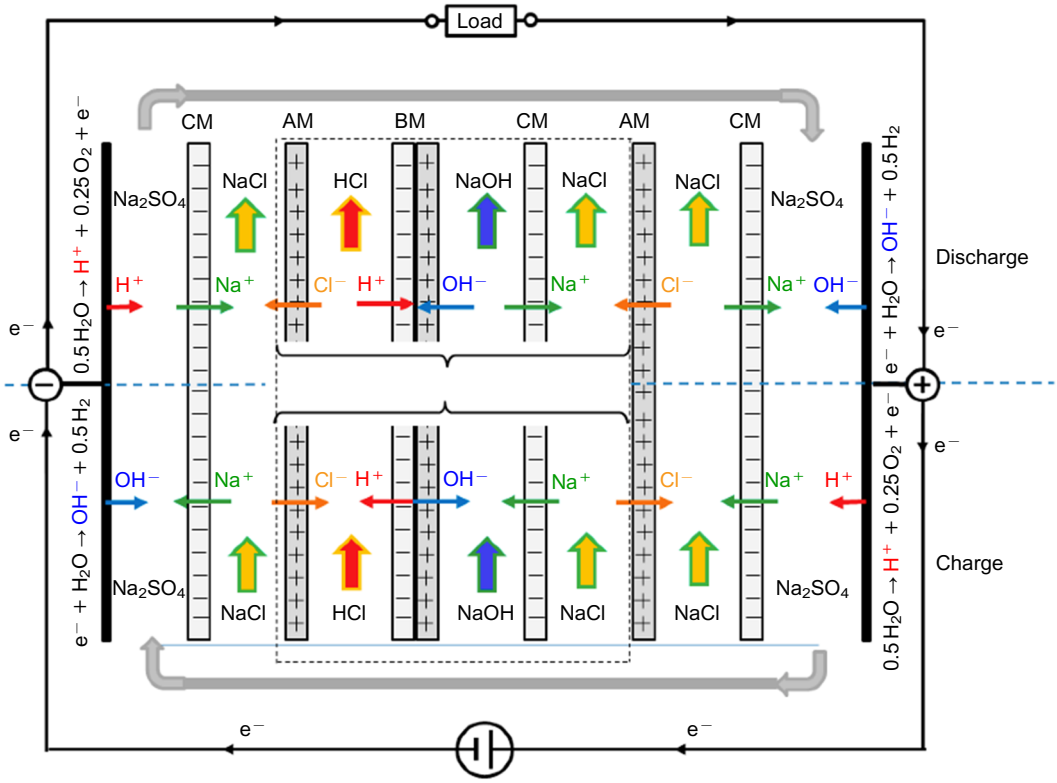


Figure 10. Scheme of three-membrane acid–base RFB. Reproduced from Ref. 131 with the permission of MDPI.

base battery with the Nafion 112 membrane, two electrolyte solutions (0.1 – 1 M NaOH and HCl in 2 M NaCl), a platinized gas diffusion electrode and platinized titanium mesh, and hydrogen as the redox component. The reactions taking place on the electrodes in this system are described by Eqns (43) and (44). The power density varied from 19 (48 mA cm^{-2} and 20 °C) to 25 mW cm^{-2} (63 mA cm^{-2} and 50 °C) for the highest concentration. Charge – discharge cycling was carried out at a current density of 25 mA cm^{-2}; in the case of 1 M acid and alkali solutions, the coulombic efficiency was approximately 95% and the energy efficiency was 55%.

The reaction on the negative electrode

$$H_2 + 2OH^- \leftrightarrows 2H_2O + 2e^- \quad (43)$$

The reaction on the positive electrode

$$2H_3O^+ + 2e^- \leftrightarrows H_2 + 2H_2O \quad (44)$$

The theoretical energy density of an acid–base battery using 1, 4 and 6 M HCl, NaOH and NaCl solutions is 23, 100 and 153 W h L^{-1}. Irrespective of the design, acid–base flow batteries have a number of advantages over classic RFBs:

(1) low cost of electrolytes — acid, alkali and salt solutions; theoretically it is possible to use pretreated seawater as the electrolyte;

(2) high solubility of electrolytes in water, *e.g.*, the solubility of HCl is 13.75 M, that of NaCl is 6.1 M and that of NaOH is 20 M;

(3) low toxicity of solutions of electroactive components;

(4) in a design with a bipolar membrane, the battery composed of single MEAs still has in total two electrodes.[131]

The key drawbacks of acid–base batteries are as follows:

(1) a considerable drawback of acid–base battery with a bipolar membrane is the limitation on the discharge current density caused by separation of the bipolar membrane into layers. At high discharge current densities, the protons and hydroxide anions recombine so rapidly than resulting water has no time to diffuse from the membrane to the electrolyte bulk;

(2) the undesirable transfer of electrolyte components through ion-exchange membranes has an adverse effect on the battery performance. This effect is most pronounced at the initial and final stages of charging and discharge where the concentration gradient of electroactive components is maximized. In the case of batteries with bipolar membranes, this adverse effect is aggravated by the fact that the battery discharge time increases due to low current densities;

(3) the energy capacity is moderate due to too large volume of electrolytes (for electrolyte tanks). The energy storage capacity can be increased by increasing the concentration of electrolytes; however, this enhances the undesirable transfer of electrolyte components and the membrane stability problem;

(4) the voltaic efficiency of the existing batteries is relatively low, which may be attributed to the relatively high internal resistance of the batteries (three membranes per cell).

Although the concept of acid – base battery has been known for long, the number of studies on this subject is moderate. For this reason and because of the presence of unsolved problems, this RFB has not yet been commercialized. However, in 2020, batteries composed of 5 and 20 single cells[131] with an active surface area of 100 cm^2 based on the previously studied single cell of acid–base RFB[132] were reported. The authors used 1 M HCl and NaOH, 0.5 M NaCl and 0.25 M Na_2SO_4 solutions (2, 2, 2 and 1.5 L, respectively). The power density of the 20-cell battery was 3 mW cm^{-2} for 10 mA cm^{-2} current density and the absolute power was 6 W with a voltaic efficiency of 36%.[131] In the same year, another research group reported batteries composed of 5, 10, 20, 30 and 38 three-membrane MEAs with an electrode surface area of 100 cm^2.[135] DSA electrodes were used; the concentrations of HCl and NaOH solutions were varied from 0.2 to 1 M. The highest power density of the 10 MEA battery with 1 M electrolyte solutions amounted to 5.1 mW cm^{-2} at 10 mA cm^{-2}.

Other RFBs using auxiliary processes. It is necessary to briefly mention some other types of RFBs that utilize not only redox reactions to generate electricity.

For example, this refers to photoelectrochemical RFBs that comprise a photoanode on which an electron – hole pair appears and triggers oxidation of the redox component in the electrolyte.[136 – 140] They can directly convert solar energy to chemical energy, without the stage of conversion to electrical energy; therefore, they are considered to be a more cost-effective substitute for conventional photovoltaic systems. Furthermore, photoelectrochemical RFBs possess the principal advantage of RFBs, that is, the independent scalability of power and capacity characteristics. The electrolytes traditionally used in photoelectrochemical RFBs represent various organic compounds, AQDS, TEMPO or viologen derivatives, demonstrating specific powers of up to 150 mW cm^{-2} and efficiency of radiation conversion to chemical energy of up to 14%.

In thermally regenerative RFBs, the waste anolyte is regenerated in the distillation column at 90 – 130 °C.[141 – 143] In the European industry sector, hundreds of TW h of potential energy stored as waste heat is lost every year. The use of thermally regenerative RFBs appears to be an environmentally friendly way for converting this energy to electricity. Unlike other thermally regenerative units operating at temperatures above 200 °C, thermally regenerative RFBs are meant for the use of low-potential thermal energy (90 – 130 °C). Currently, the best prototypes of thermally regenerative RFBs show an energy density of up to 1.28 W h L^{-1}, power density of up to 30 mW cm^{-2} and thermoelectric conversion efficiency of up to 3.8%.

Finally, mention should be made of the RFB concept combined with microbial fuel cells in which charging of one or several electrolytes takes place in a bioelectrochemical cell and involves exoelectrogenic bacteria. In the future, this approach would reduce the cost of electricity compared with classic RFBs, since it allows storage of chemical energy generated from biomass rather than by applying an external voltage. Currently, it was shown that AQDS can be reduced to $AQDSH_2$ with the subsequent use of the solution as the catholyte.[144] The maximum power density was 32.6 mW cm^{-2} and the coulombic efficiency was 20%.

Thus, type II hybrid RFBs use the general principles of flow batteries with electrical energy conversion to chemical energy *via* electrochemical reactions of compounds dissolved in liquid electrolytes, but this concept is substantially

modified, in particular, using various design innovations, *e.g.*, by using several MEAs or additional electrolyte circuits.

Often this leads to considerable improvement of some characteristics of these energy storage devices in comparison with RFBs. For example, hydrogen bromate RFBs have markedly higher power densities owing to the use of autocatalytic cycles; redox mediator lithium flow batteries theoretically allow an increase in the stored energy density by several orders of magnitude; and suspension RFBs can considerably reduce the capital cost as they do not require expensive electrode materials. However, none of RFBs of type II has been commercialized; they are only at the laboratory stage due to serious complications associated with these approaches.

4. Note added in proof

As the review was prepared, several significant publications appeared. It is necessary to consider these publications in brief.

Yao *et al.*[145] reported key characteristics of RFBs (power density, stored energy density, energy efficiency, *etc.*) and procedures for determination of these characteristics, which is a useful illustration to analysis of the relationships between the performance of various types of RFBs that we present in Section 2.3.6.

Economic analysis of the key factors and risks determining the availability and cost of vanadium electrolytes for VRFBs reported by Ciotola *et al.*[146] presents a brilliant rationale for the search for other types of VRFBs apart from the well-studied and commercialized ones (see Section 3.1.1).

Hu *et al.*[147] proposed a new organic anolyte based on the viologen derivative, in which the pyridine rings were separated by a benzene ring; the idea of this study reasonably supplements the studies described in the part 'Electrolytes based on viologens and TEMPO', Section 3.1.5. The introduction of a benzene ring between the pyridine rings violates the conjugation in the system; as a result, the new molecule can undergo reversible two-electron redox reactions. When a 0.5 M solution of this compound was used as the anolyte and a TEMPO derivative was used as the catholyte, the following key characteristics of RFB were attained: standard cell potential of 1.73 V; specific capacity of 20 A h L^{-1}; and energy efficiency of approximately 81% at a charge – discharge current density of 80 mA cm^{-2}. Regarding the set of these characteristics, the tested RFB is superior to the analogues described in the part 'Electrolytes based on viologens and TEMPO' of the review.

Chen *et al.*[148] proposed an idea that develops the semisolid electrode RFB concept (see the relevant part of Section 3.3.2). The authors made an attempt to stop using conductive additives in suspension electrolytes of RFBs. Instead of planar electrodes, they used three-dimensional electrodes combined with current collectors and made of carbon felt. This eliminated the need for conductive additives that served as the electrode distributed throughout the suspension and on the surface of which redox reactions took place. This innovation markedly reduced the viscosity of the suspension and, accordingly, the power consumption for pumping. A lithium flow battery using such a single-component suspension as an electrolyte demonstrated a high stored energy density (230 W h L^{-1}) and a coulombic efficiency that was high for this type of RFB (approximately 95% after 100 charge – discharge cycles).

Finally, the publication of Kim *et al.*[149] supplements the part 'Acid–base RFB', Section 3.3.4. The authors proposed a new design of acid – base RFB using an asymmetric bipolar membrane. This increased the power density to 3.85 mW cm^{-2} with the use of 2 M electrolyte solutions; the results of long-term charge – discharge cycling was demonstrated for 60 cycles; the coulombic, voltaic and energy efficiency were 98.9, 56.1 and 55.5%, respectively, for a current density of 4 mA cm^{-2}.

5. Conclusion

Redox flow batteries are a promising type of energy storage devices that appear especially appropriate in the power grid nodes where a balance is required between irregular electrical energy production and consumption rates. Among all sorts of RFBs, vanadium RFBs have been most studied. They most fully disclose the benefits inherent in flow batteries in comparison with other types of CPSs: independent scalability of the power and capacity characteristics of the storage system, the absence of self-discharge, long lifetime, *etc.*

However, both vanadium batteries and other types of classic RFBs in which the electricity is stored and released as a result of electrochemical transformations of redox-active compounds dissolved in liquid electrolytes have some drawbacks, first of all, relatively low stored energy density, in comparison with other types of CPSs, and limited power density, which complicates the possibility of handling pulses and short-term changes of charge and discharge currents. These features of classic RFBs and desire to minimize the capital and operating costs of the manufacture and use of RFB-based energy storage systems stimulate the development of various types of hybrid batteries combining the general principles (and hence the benefits) of RFBs with half-cells of other types of CPSs.

In this review, these types of RFBs were split into two groups. The designs in which one of the redox-active components, at least in one redox state, occurs in a different phase and/or crosses the interface during operation of the device were classified as type I hybrid RFBs. These RFBs possess certain advantages over the classic redox batteries; however, in the whole set of characteristics, they are currently inferior to the vanadium redox flow batteries. Type II hybrid RFBs comprise solutions that can hardly be assigned to either classic RFBs or type I hybrid RFBs, because they fundamentally differ from the original concept of redox batteries. In some key characteristics such as the stored energy density or power density, these batteries markedly surpass classic RFBs; however, their practical implementation is currently faced with a number of unsolved problems, *e.g.*, selection of the optimal MEA design, electrode materials, electrolyte circulation regime, *etc.*

Currently, the proportion of RFBs among all installed energy storage devices is moderate; however, in view of strengthening of the role of renewable energy engineering and implementation of distributed power grids and progress in the design and optimization of redox batteries, the role of RFBs in the energy storage would steadily grow, in particular, at the expense of hybrid designs.

This study was supported by the Russian Foundation for Basic Research (Project No. 19-13-50266, Expansion). The collection and analysis of published sources on hybrid RFBs were performed within the State Assignment (state registration AAAA-A19-119061890019-5, subject 0089-2019-0007) using the resources of the Competence Center of the National Technology Initiative at the Institute of Problems of Chemical Physics, Russian Academy of Sciences.

6. List of acronyms and designations

ABRFB — anthraquinone bromine redox flow battery,
AQDS — 9,10-anthraquinone-2,7-disulfonic acid,
AQS — anthraquinonesulfonic acid,
CPS — chemical power source,
JIT — Just-in-time principle — principle of necessity of energy consumption at the time it is produced,
KB — Ketjen Black, a carbon support (suspension of carbon nanoparticles)
LiTFSI — lithium bis(trifluoromethanesulfonyl)imide,
MEA — membrane electrode assembly,
MV — methyl viologen,
PANI — polyaniline,
RFB — redox flow battery,
SOC — state of charge,
TEMPO — (2,2,6,6-tetramethylpiperidin-1-yl)oxyl,
TMPD — tetramethylphenylenediamine.
VRFB — vanadium redox flow battery.

References

1. *Global Energy Transformation: A roadmap to 2050* ; https://www.irena.org/publications/2019/Apr/Global-energy-transformation-A-roadmap-to-2050-2019Edition (last accessed May 25, 2021)
2. *Electricity Storage and Renewables: Costs and Markets to 2030*; https://www.irena.org/publications/2017/Oct/Electricity-storage-and-renewables-costs-and-markets (last accessed May 25, 2021)
3. A.Berrada, K.Loudiyi. In *Gravity Energy Storage*. (Amsterdam: Elsevier, 2019). P. 186
4. A.Z.Weber, M.M.Mench, J.P.Meyers, P.N.Ross, J.T.Gostick, Q.Liu. *J. Appl. Electrochem.*, **41**, 1137 (2011)
5. M.Skyllas-Kazacos, G.Kazacos, G.Poon, H.Verseema. *Int. J. Energy Res.*, **34**, 182 (2010)
6. M.Bartolozzi. *J. Power Sources*, **27**, 219 (1989)
7. P.Alotto, M.Guarnieri, F.Moro. *Renew. Sust. Energ. Rev.*, **29**, 325 (2014)
8. L.F.Arenas, C.Ponce de León, F.C.Walsh. *J. Energy Storage*, **11**, 119 (2017)
9. Y.Ding, C.Zhang, L.Zhang, Y.Zhou, G.Yu. *Chem. Soc. Rev.*, **47**, 69 (2018)
10. Q.Huang, Q.Wang. *Chempluschem*, **80**, 312 (2015)
11. C.Ponce de Leon, A.Frias-Ferrer, J.Gonzalez-Garcia, D.A.Szanto, F.C.Walsh. *J. Power Sources*, **160**, 716 (2006)
12. J.Noack, N.Roznyatovskaya, T.Herr, P.Fischer. *Angew. Chem.* **54**, 9776 (2015)
13. J.Winsberg, T.Hagemann, T.Janoschka, M.D.Hager, U.S.Schubert. *Angew. Chem.*, **56**, 686 (2017)
14. Y.Ding, C.Zhang, L.Zhang, Y.Zhou, G.Yu. *Chem.*, **5**, 1964 (2019)
15. S.Zhang, W.Guo, F.Yang, P.Zheng, R.Qiao, Z.Li. *Batteries & Supercaps*, **2**, 627 (2019)
16. V.Singh, S.Kim, J.Kang, H.R.Byon. *J. NanoR*, **12**, 1988 (2019)
17. R.Chen. *CurrOpin. Electrochem.*, **21**, 40 (2020)
18. T.N.Pham-Truong, Q.Wang, J.Ghilane, H.Randriamahazaka. *Chemsuschem.*, **13**, 2142 (2020)
19. L.Hu, L.Gao, M.Di, X.Jiang, X.Wu, X.Yan, X.Li, G.He. *Energy Storage Mater.*, **34**, 648 (2021)
20. A.D.Kachan. In *Rezhimy Raboty i Ekspluatatsii Teplovykh Elektricheskikh Stantsii. (Modes of Work and Operation of Thermal Power Plants)*. (Minsk: Izd. Vysshaya Shkola, 1978). P. 288
21. A.Schäfer, H.Schuster, U.Kasper, A.Moser. In *Electrochemical Energy Storage for Renewable Sources and Grid Balancing*. (Amsterdam: Elsevier, 2015). P. 23
22. *New Energy Outlook 2019*; https://about.bnef.com/new-energy-outlook/ (last accessed May 25, 2021)
23. *The Causes and Effects of Negative Power Prices*; https://www.cleanenergywire.org/factsheets/why-power-prices-turn-negative (last accessed May 25, 2021)
24. *Negative Electricity Market Prices*; https://set.kuleuven.be/ei/images/negative-electricity-market-prices (last accessed May 25, 2021)
25. K.Mongird, V.Fotedar, V.Viswanathan, V.Koritarov, P.Balducci, B.Hadjerioua, J.Alam. In *Energy Storage Technology and Cost Characterization Report*. (U.S. Department of Energy, United States, 2019). P. 120
26. M.E.Amiryar, K.R.Pullen. *Appl. Sci.*, **7**, 286 (2017)
27. *New Flywheel Raises Hopes for Energy Storage Breakthrough*; https://www.ajot.com/news/flywheel-energy-storage-market-new-flywheel-raises-hopes-for-energy-storage-breakthrough (last accessed May 25, 2021)
28. A.G.Ter-Gazarian. In *Energy Storage for Power Systems*. (2nd Edn). (London: Peter Peregrinus Ltd., 2011). P. 100
29. *Bloomberg NEF: Lithium-Ion Battery Cell Densities Have Almost Tripled Since 2010*; https://cleantechnica.com/2020/02/19/bloombergnef-lithium-ion-battery-cell-densities-have-almost-tripled-since-2010/ (last accessed May 25, 2021)
30. *New Jersey Energy Storage Analysis (ESA Final Report, May 23, 2019*; https://www.bpu.state.nj.us/bpu/pdf/commercial/New%20Jersey%20ESA%20Final%20Report%2005-2-3-2019.pdf (last accessed May 25, 2021)
31. *About NAS Batteries*; https://www.ngk-insulators.com/en/product/nas/about/index.html (last accessed May 25, 2021)
32. *Sodium Sulfur Battery In Abu Dhabi Is World's Largest Storage Device*; https://cleantechnica.com/2019/02/03/sodium-sulfur-battery-in-abu-dhabi-is-worlds-largest-storage-device/ (last accessed May 25, 2021)
33. G.J.May, A.Davidson, B.Monahov. *J. Energy Storage*, **15**, 145 (2018)
34. T.Ma, H.Yang, L.Lu. Appl. Energy, **153**, 56 (2015)
35. X.Liu, D.Ren,H.Hsu,X.Feng,G.-L.Xu, M.Zhuang, H.Gao, L.Lu, X.Han, Z.Chu, J.Li, X.He, K.Amine, M.Quyang. *Joule*, **2**, 2047 (2018)
36. C.Minke, U.Kunz, T.Turek. *J. Power Sources*, **361**, 105 (2017)
37. *DOE OE Global Energy Storage Database*; https://www.sandia.gov/ess-ssl/global-energy-storage-database-home/ (last accessed May 25, 2021)
38. *Green Globe: China Starts Building World's Largest Vanadium Flow Battery*; https://www.spglobal.com/marketintelligence/en/news-insights/trending/1sgv2yl4jn3r-r18pibt0g2 (last accessed May 25, 2021)

39. *Global Vanadium Redox Battery (VRB) (All-vanadium Redox Flow Batteries) Market 2019 by Manufacturers, Regions, Type and Application, Forecast to 2024*; https://www.absolutereports.com/global-vanadium-redox-battery-vrb-all-vanadium-redox-flow-batteries-market-13985469 (last accessed May 25, 2021)
40. Patent US 3996064 (1976)
41. Patent US 25630927 (1988)
42. M.Skyllas-Kazacos, F.Grossmith. *J. Electrochem. Soc.*, **134**, 2950 (1987)
43. M.Rychcik, M.Skyllas-Kazacos. *J. Power Sources*, **22**, 59 (1988)
44. C.Choi, S.Kim, R.Kim, Y.Choi, S.Kim, H.-Y.Jung, J.H.Yang, H.-T.Kim. *Renew. Sust. Energ. Rev.*, **69**, 263 (2017)
45. D.Bryans, V.Amstutz, H.H.Girault, L.E.A.Berlouis. *Batteries*, **4**, 54 (2018)
46. F.Rahman, M.Skyllas-Kazacos. *J. Power Sources*, **189**, 1212 (2009)
47. J.Houser, A.Pezeshki, J.Clement, D.Aaron, M.M.Mench. *J. Power Sources*, **351**, 96 (2017)
48. D.Aaron, C.-N.Sun, M.Bright, A.B.Papandrew, M.M.Mench, T.A.Zawodzinski. *ECS Electrochem. Lett.*, **2**, 29 (2013)
49. R.D.Pichugov, D.V.Konev, M.M.Petrov, A.E.Antipov, P.A.Loktionov, L.Z.Abunaeva, A.A.Usenko, M.A.Vorotynstev. *ChemPlusChem*, **85**, 1919 (2020)
50. A.T.Glazkov, A.E.Antipov, D.V.Konev, R.D.Pichugov, M.M.Petrov, N.V.Kartashova, P.A.Loktionov, J.M.Averina, I.I.Plotko. *Data Brief*, **31**, 105840 (2020)
51. Patent JP 6124172 (1986)
52. L.H.Thaller. In *Electrically Rechargeable Redox Flow Cells. NASA Technical Memorandum. Ninth Intersociety Energy Conversion Engineering Conference*. (San Francisco, California, 1974). P. 8
53. L.H.Thaller. In *Redox Flow Cell Energy Storage Systems. NASA Technical Memorandum*. (Washington, DC: U.S. Department of Energy Conservation and Renewable Energy Division of Energy Storage Systems, , 1979). P. 14
54. Y.K.Zeng, T.S.Zhao, X.L.Zhou, L.Zeng, L.Wei. *Appl. Energy*, **182**, 204 (2016)
55. Y.K.Zeng, X.L.Zhou, L.Zeng, X.H.Yana, T.S.Zhao. *J. Power Sources*, **327**, 258 (2016)
56. Y.K.Zeng, T.S.Zhao, L.An.X.L.Zhou, L.Wei. *J. Power Sources*, **300**, 438 (2015)
57. E.Hollax, D.Sh.Cheng. *Carbon*, **23**, 655 (1985)
58. C.D.Wu, D.A.Scherson, E.J.Calvo, E.B.Yeager, M.A.Reid. *J. Electrochem. Soc.*, **133**, 2109 (1986)
59. *Long-duration, Grid-scale Iron-chromium Redox Flow Battery Systems*; https://www.sandia.gov/ess-ssl/docs/pr_conferences/2014/Thursday/Session7/01_Nevins_Sheri_IRON-CHROMIUM_REDOX.pdf (last accessed May 25, 2021)
60. Patent US 4485154 (1984)
61. H.Zhang. *In Advances in Batteries for Medium and Large-scale Energy Storage Types and Applications*. (Woodhead Publishing, UK, 2014). P. 634
62. Z.Li, G.Weng, Q.Zou, G.Cong, Y.-C.Lu. *Nano Energy*, **30**, 283 (2016)
63. *Regenesys Utility Scale Energy Storage, Project Summary*; https://inis.iaea.org/search/search.aspx?orig_q=RN:36018156 (last accessed May 25, 2021)
64. B.Huskinson, M.P.Marshak, C.Suh, S.Er, M.R.Gerhardt, C.J.Galvin, X.Chen, A.Aspuru-Guzik, R.G.Gordon, M.J.Aziz. *Nature (London)*, **505**, 195 (2014)
65. T.Carney, S.J.Collins, J.S.Moore, F.R.Brushett. *Chem. Mater.*, **29**, 4801 (2017)
66. Q.Chen, L.Eisenach, M.J.Aziz. *J. Electrochem. Soc.*, **163**, A5057 (2016)
67. Q.Chen, M.R.Gerhardt, L.Hartle, M.J.Aziz. *J. Electrochem. Soc.*, **163**, A5010 (2016)
68. M.R.Gerhardt, L.Tong, R.Gómez-Bombarelli, Q.Chen, M.P.Marshak, C.J.Galvin, A.Aspuru-Guzik, R.G.Gordon, M.J.Aziz. *Adv. Energy Mater.*, **7**, 1601488 (2017)
69. A.Khataee, K.Wedege, E.Drazevic, A.Bentien. *J. Mater. Chem. A*, **5**, 21875 (2017)
70. Z.Yang, L.Tong, D.P.Tabor, E.S.Beh, M.-A.Goulet, D.D.Porcellinis, A.Aspuru-Guzik, R.G.Gordon, M.J.Aziz. *Adv. Energy Mater.*, **8**, 1702056 (2018)
71. C.Wang, Z.Yang, Y.Wang, P.Zhao, W.Yan, G.Zhu, L.Ma, B.Yu, L.Wang, G.Li, J.Liu, Z.Jin. *ACS Energy Lett.*, **3**, 2404 (2018)
72. K.Lin, Q.Chen, M.R.Gerhardt, L.Tong, S.B.Kim, L.Eisenach, A.W.Valle, D.Hardee, R.G.Gordon, M.J.Aziz, M.P.Marshak. *Science*, **349**, 1529 (2015)
73. D.G.Kwabi, K.Lin, Y.Ji, E.F.Kerr, M.-A.Goulet, D.D.Porcellinis, D.P.Tabor, D.A.Pollack, A.Aspuru-Guzik, R.G.Gordon, M.J.Aziz. *Joule*, **2**, 1894 (2018)
74. T.Liu, X.L.Wei, Z.M.Nie, V.Sprenkle, W.Wang. *Adv. Energy Mater.*, **6**, 1501449 (2016)
75. E.S.Beh, D.D.Porcellinis, R.L.Gracia, K.T.Xia, R.G.Gordon, M.J.Aziz. *ACS Energy Lett.*, **2**, 639 (2017)
76. J.Luo, B.Hu, C.Debruler, T.L.Liu. *Angew. Chem., Int. Ed.*, **57**, 231 (2018)
77. B.Liu, C.W.Tang, H.Jiang, G.Jia, T.Zhao. *J. Power Sources*, **477**, 228985 (2020)
78. T.Janoschka, N.Martin, M.D.Hager, U.Schubert. *Angew. Chem., Int. Ed.*, **55**, 46 (2016)
79. T.Janoschka, N.Martin, U.Martin, C.Friebe, S.Morgenstern, H.Hiller, M.D.Hager, Ulrich S. Schubert. *Nature (London)*, **527**, 78 (2015)
80. Patent US 312802 (1885)
81. G.P.Rajarathnam, A.M.Vassallo. In *Zinc/Bromide Battery Development – Phase III*. (Netherlands: Elsevier, 1984). P. 324
82. D.Linden, T.B.Reddy. In *Handbook of Batteries*. (New York: The McGraw-Hill Companies, 2002). P. 39.1
83. *ZBM2 Zinc-bromine Flow Battery*; https://www.redflow.com/products/redflow-zbm2/ (last accessed May 25, 2021)
84. *The Future of Storage is Long*; https://www.primuspower.com/en/ (last accessed May 25, 2021)
85. P.C.León, F.C.Walsh. In *Encyclopedia of Electrochemical Power Sources*. (Netherlands: Elsevier, 2009). P. 487
86. B.Beverskog, I.Puigdomenech. *Corros Sci*, **39**, 107 (1997)
87. GOST 12.1.005-88. *Sistema Standartov Bezopasnosti Truda (SSBT). Obshchie Sanitarno-Gigienicheskie Trebovaniya k Vozdukhu Rabochei Zony. [Occupational Safety Standards System (OSSS). General Sanitary and Hygienic Requirements for the Air of the Working Area]*
88. K.Cedzynska. *Electrochim. Acta*, **8**, 971 (1995)

89. Z.Xu, Q.Fan, Y.Li, J.Wang, P.D.Lund. *Renew. Sustain. Energy Rev.*, **127**, 109838 (2020)
90. J.Winsberg, T.Janoschka, S.Morgenstern, T.Hagemann, S.Muench, G.Hauffman, J.-F.Gohy, M.D.Hager, U.S.Schubert. *Adv. Mater.*, **28**, 2238 (2016)
91. B.Li, Z.Nie, M.Vijayakumar, G.Li, J.Liu, V.Sprenkle, W.Wang. *Nat. Commun.*, **6**, 6303 (2015)
92. X.Wei, W.Xu, M.Vijayakumar, L.Cosimbescu, T.Liu, V.Sprenkle, W.Wang. *Adv. Mater.*, **26**, 7649 (2014)
93. K.Takechi, Y.Kato, Y.Hase. *Adv. Mater.*, **27**, 2501 (2015)
94. V.Livshits, A.Ulus, E.Peled. *Electrochem. Commun.*, **8**, 1358 (2006)
95. K.T.Cho, P.Albertus, V.Battaglia, A.Kojic, V.Srinivasan, A.Z.Weber. *Energy Technol.*, **1**, 596 (2013)
96. *Energy storage: EnStorage (Israel), Partner of Areva and Schneider Electric, is prensent at COP21*; https://www.israelscienceinfo.com/en/energie/stockage-de-l-energie-enstorage-israel-partenaire-dareva-et-de-schneider-electric-participe-a-cop21/ (last accessed May 25, 2021)
97. Patent US 8968961 (2015)
98. Patent US 9012104 (2015)
99. G.L.Soloveichik. *Chem. Rev.*, **115**, 11533 (2015)
100. Yu.V.Tolmachev. *Russ. J. Electrochem.*, **50**, 301 (2014)
101. Y.V.Tolmachev, A.Piatkivskyi, V.V.Ryzhov, D.V.Konev, M.A.Vorotyntsev. *J. Solid State Electrochem.*, **19**, 2711 (2015)
102. M.A.Vorotyntsev, A.E.Antipov, D.V.Konev. *Pure Appl. Chem.*, **89**, 1429 (2017)
103. J.P.Simmons, W.F.Waldeck. *J. Am. Chem. Soc.*, **53**, 1725 (1931)
104. W.M.Haynes. In *CRC Handbook of Chemistry and Physics*. (CRC Press, US, 2014)
105. T.Mussini, P.Longhi. In *Standard Potentials in Aqueous Solutions*. (IUPAC, 1985). P. 5
106. Y.Nonobe. *IEEJ T. Electr. Electr.*, **12**, 5 (2017)
107. A.D.Modestov, D.V.Konev, O.V.Tripachev, A.E.Antipov, Y.V.Tolmachev, M.A.Vorotyntsev. *Energy Tech.*, **6**, 242 (2017)
108. Y.G.Zhu, Y.Du, C.Jia, M.Zhou, L.Fan, X.Wang, Q.Wang. *J. Am. Chem. Soc.*, **18**, 6286 (2017)
109. Q.Huang, J.Yang, C.B.Ng, C.Jia, Q.Wang. *Energy Environ. Sci.*, **9**, 917 (2016)
110. C.Jia, F.Pan, Y.G.Zhu, Q.Huang, L.Lu, Q.Wang. *Sci. Adv.*, **1**, 1500886 (2015)
111. M.Zhou, Y.Chen, M.Salla, H.Zhang, X.Wang, S.R.Mothe, Q.Wang. *Ang. Chem., Int. Ed.*, **59**, 14286 (2020)
112. Y.Preger, M.R.Johnson, S.Biswas, C.W.Anson, T.W.Root, S.S.Stahl. *ACS Energy Lett.*, **5**, 5, (2020)
113. Y.Cheng, X.Wang, S.Huang, W.Samarakoon, S.Xi, Y.Ji, H.Zhang, F.Zhang, Y.Du, Z.Feng, S.Adams, Q.Wang. *ACS Energy Lett.*, **4**, 3028 (2019)
114. Y.Zhao, S.Si, C.Liao. *J. Power Sources*, **241**, 449 (2013)
115. W.Yan, C.Wang, J.Tian, G.Zhu, L.Ma, Y.Wang, R.Chen, Y.Hu, L.Wang, T.Chen, J.Ma, Z.Jin. *Nat. Commun.*, **10** (2019)
116. M.Duduta, B.Ho, V.C.Wood, P.Limthongkul, V.E.Brunini, W.C.Carter, Y.-M.Chiang. *Adv. Energy Mater.*, **1**, 511 (2011)
117. Z.Li, K.C.Smith, Y.Dong, N.Baram, F.Y.Fan, J.Xie, P.Limthongkul, W.C.Cartera, Y.-M.Chiang. *Phys. Chem. Chem. Phys.*, **15**, 15833 (2013)
118. F.Yang, S.M.A.Mousavie, T.K.Oh, T.Yang, Y.Lu, C.Farley, R.J.Bodnar, L.Niu, R.Qiao, Z.Li, *Adv. Energy Mater.*, **8**, 1802869 (2018)
119. H.Chen, Q.Zou, Z.Liang, H.Liu, Q.Li, Y.-C.Lu. *Nat Commun.*, **6** (2015)
120. H.Jiang, L.Wei, X.Fan, J.Xu, W.Shyy, T.Zhao. *Sci. Bull.*, **64**, 270 (2019)
121. C. R. Dennison, H.Vrubel, V.Amstutz, P.Peljo, K.E.Toghill, H.H.Girault. *Chimia*, **69**, 753 (2015)
122. V.Amstutz, K.E.Toghill, F.Powlesland, H.Vrubel, C.Comninellis, X.Hu, H.H. Girault. *Energy Environ. Sci.*, **7**, 2350 (2014)
123. P.Peljo, H.Vrubel, V.Amstutz, J.Pandard, J.Morgado, A.Santasalo-Aarnio, D.Lloyd, F.Gumy, C.R. Dennison, K.E.Toghilld, H.H.Girault. *Green Chem.*, **18**, 1785 (2016)
124. J.Piwek, C.R.Dennison, E.Frackowiak, H.Girault, A.Battistel. *J. Power Sources*, **438**, 227029 (2019)
125. F.DeKörösy, E.Zeigerson. *Isr. J. Chem.*, **9**, 483 (1971)
126. F.L.Ramp. *Nature (London)*, **278**, 335 (1979)
127. A.T.Emren, V.J.M.Holmstrom. *Energy*, **8**, 277 (1983)
128. E.K.Zholkovskij, M.C.Müller, E.Staude. *J. Membr. Sci.*, **141**, 231 (1998)
129. J.Pretz, E.Staude. *Ber: Bmenges. Phys. Chem.*, **102**, 676 (1998)
130. A.Saez, V.Montiel, A.Aldaz. *Int. J. Hydrog. Energy*, **41**, 17801 (2016)
131. J.Xia, G.Eigenberger, H.Strathmann, U.Nieken. *Processes*, **8**, 99 (2020)
132. W.J.van Egmond, M.Saakes, I.Noor, S.Porada, C.J.N.Buisman, H.V.M.Hamelers. *Int. J. Energy Res.*, **42**, 1524 (2018)
133. J.Xia, G.Eigenberger, H.Strathmann, U.Nieken. *J. Membr. Sci.*, **56**, 157 (2018)
134. J.-H.Kim, J.-H.Lee, S.Maurya, S.-H.Shin, J.-Y.Lee, I.S.Chang, S.-H.Moon. *Electrochem. Commun.*, **72**, 157 (2016)
135. A.Zaffora, A.Culcasi, L.Gurreri, A.Cosenza, A.Tamburini, M.Santamaria, G.Micale. *Energies*, **13**, 5510 (2020)
136. W.Li, H.-C.Fu, Y.Zhao, J.-H.He, S.Jin. *Chem.*, **4**, 2644 (2018)
137. S.Liao, X.Zong, B.Seger, T.Pedersen, T.Yao, C.Ding, J.Shi, J.Chen, C.Lia. *Nat. Commun.*, **7**, 11474 (2016)
138. W.Li, H.-C.Fu, L.Li, M.Cabán-Acevedo, J.-H.He, S.Jin. *Angew. Chem., Int. Ed.*, **55**, 13104 (2016)
139. W.Zhang, P.Liu, X.Zhang. *IOP Conf. Ser.: Mater. Sci. Eng.*, **452**, 032068 (2018)
140. A.Khataee, J.Azevedo, P.Dias, D.Ivanou, E.Dražević, A.Bentien, A.Mendes. *Nano Energy*, **62**, 832 (2019)
141. W.Wang, H.Tian, G.Shu, D.Huo, F.Zhang, X.Zhu. *J. Mater. Chem. A*, **7**, 5991 (2019)
142. X.Zhu, M.Rahimi, C.A.Gorski, B.Logan. *ChemSusChem*, **9**, 873 (2016)
143. M.Rahimi, T.Kim, C.A.Gorski, B.E.Logan. *J. Power Sources*, **373**, 95 (2018)
144. M.S.S.Santos, L.Peixoto, J.Azevedo, R.A.R.Monteiro, C.Dias-Ferreira, M.M.Alves, A.Mendes. *J. Power Sources*, **445**, 227307 (2020)
145. Y.Yao, J.Lei,Y.Shi, F.Ai, Y.C.Lu. *Nat Energy*, (2021); https://doi.ogr/10.1038/s41560-020-00772-8
146. A.Ciotola, M.Fuss, S.Colombo,W.-R.Poganietz. *J. Energy Storage*, **33**, 102094 (2021)

147. S.Hu, T.Li, M.Huang, J.Huang, W.Li, L.Wang, Z.Chen, Z.Fu, X.Li, Z.Liang. *Adv. Mater.*, **33**, 2005839 (2021)
148. H.Chen, Y.Liu, X.Zhang, Q.Lan, Y. Chu, Y.Li, Q.Wu. *J. Power Sources*, **485**, 229319 (2021)
149. J.-H.Kim, I.S.Chang, S.-H.Moon. *J. Mater. Chem. A*, (2021); https://doi.ogr/10.1039/D0TA10676C